Microbial Induced Corrosion of Various Materials in a Reclaimed Water System

by

Amber Neal

A Thesis Presented in Partial Fulfillment
of the Requirements for the Degree
Master of Science

Approved November 2022 by the
Graduate Supervisory Committee:

Morteza Abbaszadegan, Chair
Peter Fox
Absar Alum

ARIZONA STATE UNIVERSITY

December 2022

ABSTRACT

Corrosion is known to have severe infrastructure integrity implications in a broad range of industries including water and wastewater treatment and reclamation. In the U.S. alone, the total losses due to corrosion in drinking water and wastewater systems can account for economic losses as high as $80 billion dollars a year. Microbially induced corrosion is a complex phenomenon which involve various phases; 1) formation of biofilms on submerged surfaces, 2) creation of micro-environmental niches associated with biofilm growth, 3) altered availability nutrients, 4) changes in the pH and oxygen concentrations. Biofilms can harbor opportunistic or pathogenic bacteria for a long time increasing the risk of pathogen exposure for the end users.

The focus of this thesis research was to study the kinetics of microbially induced corrosion of various materials in water and reclaimed water systems. The specific objective was to assess the biofilms formation potential on stainless steel 304, stainless steel 316, galvanized steel, copper, cPVC, glass, carbon steel, and cast iron in water and reclaimed water systems. Experiments were conducted using bioreactor containers, each bioreactor housed four sampling boxes with eight partitions, dedicated to each material type coupon. One bioreactor was stationed at ASU, and one at Vistancia Aquifer Storage and Recovery (ASR) well; while three bioreactors were stationed at Butler facility, at pre-disinfection, post-UV and post-chlorination. From each location, one submerged sampling box was retrieved after 1, 3, 6 and 12 months. Time series of biofilm samples recovered from various types of coupons from different locations were analyzed using physical and culture-based techniques for quantification of biofilms and detection of

heterotrophic plate count (HPC) bacteria, *Legionella*, *Mycobacterium,* and sulfate reducing bacteria (SRB).

After one-year, galvanized steel had the highest concentration of HPC at 4.27 logs while copper had the lowest concentration of 3.08 logs of HPC. Bacterial growth data collected from the SRB tests was compiled to develop a numerical matrix using growth potential, biofilm formation potential and metal reduction potential of SRB isolates. This risk assessment matrix can be a useful tool for the water industry to evaluate the potential risk of MIC in their systems.

TABLE OF CONTENTS

Page

CHAPTER Page

LIST OF TABLES

LIST OF FIGURES

Figure Page

Figure Page

CHAPTER 1: INTRODUCTION

1.1 Introduction and Purpose

A 2002 study done by the Federal Highway Administration suggested that the cost of lost water and replacing infrastructure impacted by corrosion in U.S. drinking water and sewer systems alone equates to approximately $80 billion dollars a year (Trenchless Technology, 2019). Microbially induced corrosion (MIC) is believed to be responsible for 20% of the estimated corrosion cost (Jia et al. 2018, Makhlouf and Botello, 2018). The effective life of metal pipes can be reduced by corrosive bacteria to less than 3 years and in extreme cases, concrete structures may only last 10 years (Makhlouf and Botello, 2018). The microbes responsible for MIC are of concern because they can interfere/complement with other types of naturally occurring corrosion, resulting in further damage.

The mechanism of MIC occurs in three phases. First, a biofilm forms on a material that has been submerged in water then a change of environment within the biofilm occurs as bacteria grow (Makhlouf and Botello, 2018). These changes that occur include "chemical concentrations at the surface of the metal substrate, a decrease in pH level toward acidic, a decrease in oxygen concentration, and displacement of the corrosion potential toward more positive potentials" (Makhlouf and Botello, 2018). Lastly, degradation of the metal occurs as Iron Sulfate and iron hydroxide are produced.

While the true bio-electromechanics of MIC bacteria is largely debated there are some known facts about the occurrence of MIC. First, presence of an anode, cathode, and

electrolyte is a must for the corrosion to occur (Javaherdashti, 2018). Second, pH and temperature have an impact on the rate at which MIC occurs. Third, biofilms provide conditions supporting MIC while protecting corrosive bacteria from disinfection or unfavorable environments. Lastly, the rate-limiting factor is electron transfer (Jia et al. 2017).

Bacteria involved in MIC can cause or accelerate corrosion in almost any environment. These bacteria may be anaerobic or aerobic. Sulfur reducing bacteria (SRB) reduce sulfate to sulfur and hydrogen sulfide gas while iron oxidizing bacteria oxidize Iron (II) into Iron (III). However, there are many other bacteria which facilitate MIC such as sulfur oxidizing bacteria which produce acids including sulfuric, acetic, and succinic acid. There are also acid producing bacteria and iron reducing bacteria which may facilitate MIC, as well.

Anerobic SRB are naturally occurring in the environment wherever there are carbon substrates and sulfates available. Furthermore, “SRB can grow in a wide range of environments spanning the spectrum of pressure, temperature, salinity, and pH values found in the Earth's upper crust” (Goldhaber, 2003). Thus, they pose to be a potential problem to any type of aquatic environment or sewer system. They are notorious for producing Iron Sulfide as a biproduct along with Hydrogen Sulfide gas. The Iron Sulfide can act as a corrosive agent and as a protector of metal surfaces depending on the environmental conditions. However, in a biofilm, sessile SRB are far more corrosive than planktonic cells (Tripathi et al., 2021).

Biofilms are naturally occurring in the environment and increase the chances of bacterial survival. They adhere to surfaces using extra-polymeric substances comprising of polymers which allow for a bacterial community to thrive in a sheltered environment. Bacteria along with protozoa inside of the biofilm are protected from disinfection and unfavorable, hostile conditions. Established biofilms on metal alloys can have a severe impact on corrosion as they can metabolize the film coating of metal alloys. Mixed cultures of bacteria within the biofilm, especially those containing sulfur and iron reducing bacteria (IRB), have the ability to create an ideal environment that will accelerate corrosion rates of iron containing metals (Jia et al., 2017). When chlorides are added to the environment, not only will the biofilm help protect the bacteria inside but the pH within the biofilm may decrease as well and cause accelerated corrosion (Javaherdashti, 2018). Furthermore, biofilms can contain bacteria that are considered opportunistic waterborne pathogens, such as *Legionella* and *Mycobacterium*.

Legionella is an easily aerosolized water bacteria that can cause disease. Many who are immunocompromised are at risk of Legionnaire's disease or Pontiac Fever and in severe cases *Legionella* can cause death. In wastewater, *Legionella* is often detected and suspected of surviving inside protozoan hosts in activated sludge systems (Caicedo et al., 2016). There is also "positive correlations of *Legionella spp*. concentration with particulate chemical oxygen demand, Kjeldahl nitrogen and protein concentration" (Caicedo et al., 2016).

Mycobacterium is another opportunistic waterborne pathogen. It is commonly found in arid regions where water reclamation is common as it can cause tuberculosis,

pulmonary infections, chronic ulcers, and leprosy. In wastewater facilities it is known that non-tuberculosis *Mycobacterium* "increase in relative abundance across the chlorine disinfection step" (Amha et al. 2017). This is of particular concern because not only is *Mycobacterium* of abundance and able to survive chlorine disinfection, but it requires iron for growth and virulence.

1.2 Objectives

The objectives of this study are:

1. To study microbial induced corrosion of various materials in a reclaimed water system
    a. Biofilm formation assessment on various non-porous materials coupons
        i. stainless steel 304, stainless steel 316, galvanized steel, copper, cPVC, glass, carbon steel, and cast iron
    b. Study of microbial corrosion seasonality relevant to central Arizona
    c. Characterization of sulfur reducing bacteria activities on the coupons from the water system
    d. Development of corrosion risk index

CHAPTER 2: LITERATURE REVIEW

2.1 Corrosion Mechanisms

The mechanism in which metal corrosion occurs, especially in the presence of a bacterial biofilm, is complex and largely understudied. The main concept of metal corrosion involves an anode, which is the surface area experiencing corrosion and a cathode, which is the parts of metal that are not corroding (Javaherdashti, 2018). Largely, corrosion is simply caused by the loss or gain of electrons in an aqueous environment. When a material loses electrons an oxidation reaction occurs which is also called an anodic reaction and when electrons are gained a reduction reaction has occurred which is often called a cathodic reaction as shown below (Javaherdashti, 2018):

$$\text{Oxidation (Anodic) Reaction: } Fe \longrightarrow Fe^{2+} + e^-$$

$$\text{Reduction (Cathodic) Reaction: } 2H^+ + 2e^- \longrightarrow H_2\,(\text{gas})$$

One theory for explaining the mechanism of corrosion by SRB was introduced in 1934 by Von Wolzogen Kuhr and Van der Vlugt which is known as the "Cathodic Depolarization Theory". This theory proposes that hydrogenase is utilized by SRB to consume hydrogen which is produced during the cathodic reaction. Thus, SRB are able to reduce sulfate as shown in the following net reaction (Lv and Du, 2017):

$$4Fe + SO_4^{2-} + 4H_2O \longrightarrow FeS + 3Fe(OH)_2 + 2OH^-$$

The “biocatalytic cathodic sulfate reduction theory” was introduced in 2009 by Gu et al. to explain SRB corrosion. This theory suggests that SRB are able to reduce sulfate within their cytoplasm using elemental iron when there is a lack of carbon sources. This reaction is shown below (Lv and Du, 2017):

$$\text{Oxidation Reaction (iron oxidation): } Fe \longrightarrow Fe^{2+} + e^-$$

$$\text{Reduction Reaction: } SO_4^{2-} + 9H^+ + 8e^- \longrightarrow HS^- + 4H_2O$$

There are multiple types of corrosion enhancement by MIC that can be accelerated by MIC within a biofilm. Pitting corrosion is a localized corrosion in which bacteria penetrate a material leaving small holes. This location becomes anodic while the surrounding area is cathodic allowing for localized diffusion of ions that cause corrosion. Crevice corrosion occurs specifically in joints where there is a crevice or crack. This is common at joints or corners of metal tanks as well as around fasteners. Since these areas have low or no water flow it is an ideal area for microbes to accumulate and easily establish biofilms that result in corrosion. Stressed corrosion occurs when metal alloys are susceptible to tensile stress that causes cracking in the material during certain environmental conditions in which bacteria become imbedded to further corrode.

2.1.1 Biofilm

Biofilms occur everywhere in the environment, on all surfaces. They occur naturally and when environmental conditions are unfavorable to protect bacteria. As shown below in figure 1, this occurs when planktonic bacteria find a nutrient rich environment. Once the

bacteria adhere to the surface in moist environment, sessile cells begin to multiply. As the new biofilm grows an organic polymer matrix referred to as exopolysaccharide substance (EPS) forms to protect the bacteria.

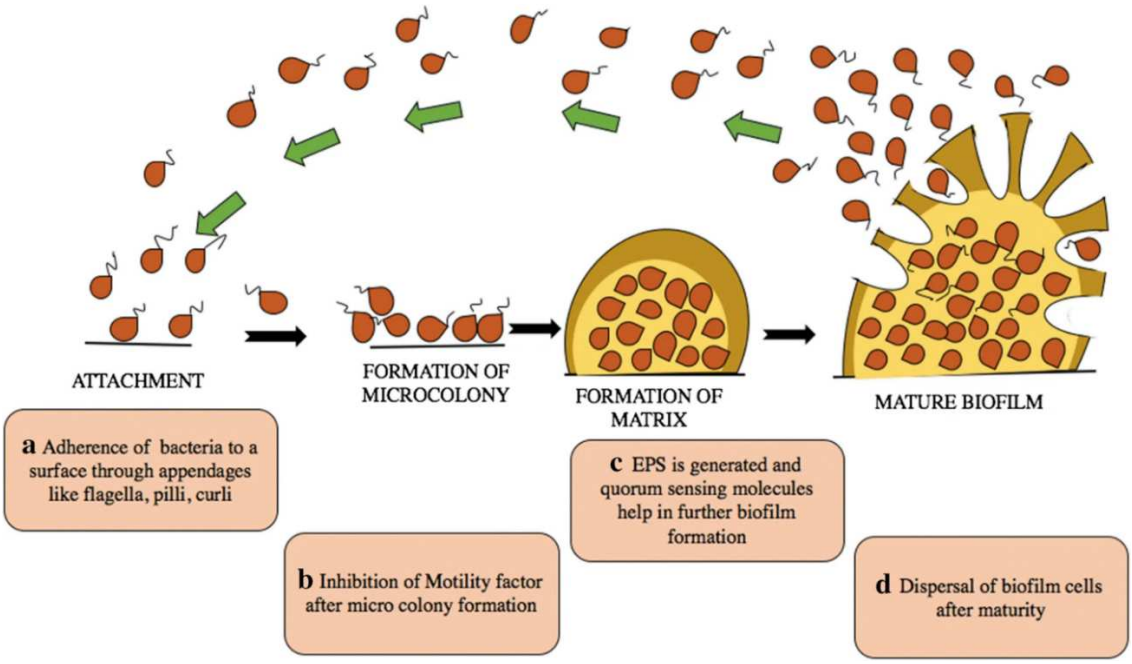

Figure 1: The life stages of biofilm formation from planktonic cells to the development of EPS in a mature biofilm (Banerjee et al., 2020).

As the biofilm forms layers of protection form as well. The internal conditions of the biofilm are more favorable and protect the bacteria from the harmful outside environment. Once multiple differentiated layers are developed, and the biofilm is mature the bacteria are well protected from disinfectants as a majority of the biofilm is comprised of EPS. At this stage of biofilm development many disinfectants, such as chlorine, fail to effectively penetrate the EPS and kill the complex bacteria matrix within the biofilm. However, even though these established biofilms compromise the

effectiveness of disinfection processes, they are used in wastewater treatment facilities to remove organic waste and break down ammonium into nitrate.

Thick, mature biofilms not only make disinfection difficult but can change the environment underneath the biofilm. As the EPS grows environmental factors underneath the biofilm may be different from the external environment. Such factors may include but are not limited to pH, temperature, oxygen levels, nutrients, and ions. This results in ennoblement of various metals and alloy (Javaherdashti, 2018).

When ennoblement of stainless steel occurs, there is a 400mV increase in the open circuit potential (Trigodet et. al. 2019). The occurrence of ennoblement combined with biofilm protection allows for an acceleration of localized corrosion. When sessile SRB are present in a biofilm just 12μm thick or more ennoblement increases pitting corrosion susceptibility at a higher rate than platonic bacteria (Javaherdashti, 2018). Other factors such as the presence of sedimentary manganese and the formation of siderophores or iron chelators produced by some bacteria, such as *Pseudomonas*, impact the occurrence of ennoblement.

2.1.2 Pitting Corrosion

Pitting corrosion is a specific type of corrosion that is localized and results in cavities in various materials. This type of corrosion is highly localized due to the anodic area being drastically smaller than the cathodic area. Pitting corrosion is the most dangerous type of corrosion because it is highly difficult to detect and monitor. The

developed pits are the result of random oxidation of a material and are typically a precursor to cracking corrosion.

2.1.3 Crevice Corrosion

Crevice Corrosion is also highly localized and occurs when two different metals are submerged in a solution that allows for an electrical connection. This occurs because one metal in the solution, which is the cathode, is protected; while the other metal, which is the anode, is corroded at an accelerated rate. The anode corrodes faster due to its higher electrical potential along with the presence of stagnant water, manganese, and biofouling deposits.

2.1.4 Stressed Cracking Corrosion

Stressed Corrosion cracking (SCC) occurs due to weakened tensile strength of a susceptible metal in a corrosive environment. When the stress on the material surpasses the tensile yield strength the material is subject to failure. The presence of biofilms containing any acid or hydrogen producing bacteria severely impacts the occurrence of SCC along with environmental factors such as pH and temperature.

2.1.5 Chlorine

Chlorine is used as a broad-spectrum oxidizing biocide used in the water treatment process. It is economical and effective at inactivating bacteria. Furthermore, it is easy to monitor chlorine residual to meet the U.S. Environmental Protection Agency's demands.

There are significant downfalls to using chlorine. It can be hazardous to humans and corrosive to metals. Chlorine will react with organic matter and create carcinogenic trihalomethanes. Chlorine also enhances MIC. The presence of chlorine may accelerate corrosion under any deposit build-up caused by natural corrosion. On stainless steels, chlorine ions damage the protective film, and with galvanized steel, chlorine will cause zinc to leach out as the metal rapidly erodes. Furthermore, chlorine will react with copper pipes to create copper (II) chloride deposits and iron create ferric chloride.

2.2 Sulfur Reducing Bacteria

Sulfur reducing bacteria are generally anerobic, however some species including *Desulfovibrio vulgaris* and *Desulfovibrio desulfuricans* can consume oxygen for energy without growth (Jia et al. 2017). SRB use sulfur compounds, including bisulfate and thiosulfate as a terminal electron acceptor but can also use elemental sulfur (Jia et al. 2017). In stressed environmental conditions, elemental iron can be used to reduce sulfate, further complicating the mechanism of corrosion by SRB (Lv and Du, 2017).

The impact of SRBs on human health can be devastating. SRBs can infect individuals that have a compromised immune system and are a frequent threat to sewer workers. In India alone, over the last three decades nearly 1000 individuals have lost their lives working in sewers (Jyoti, 2021). Some sanitary workers have lost their lives to poisonous gas production as well, including two gentlemen in North Scottsdale who

jumped down into a 15-foot sewer main to rescue an 18-year-old boy who had fallen in and could not get out on his own (The Republic, 2014).

2.2.1 *Desulfovibrio vulgaris*

D. vulgaris is a gram-negative, non-spore forming, sulfate reducing anaerobe. Due to its complex metabolic capability, it is ubiquitous in nature and toxic to majority of life. They are notorious for reducing sulfur into hydrogen sulfide gas. Furthermore, *D. vulgaris* poses a threat to the general public's health and to water facilities.

Although *D. vulgaris* is toxic to many life forms it is important to the environment's natural sulfur cycle and for remediation purposes. Its ability to reduce sulfate to sulfide accounts for over 50% of the organic carbon found in marine sediments (Tao et al., 2014). *D. vulgaris* is also capable of precipitating copper (II) and reducing some heavy metals along with thiosulfate into non-toxic forms (Tao et al., 2014).

2.3 Iron Reducing Bacteria

IRB are anaerobic bacteria that have the ability to reduce iron along with other metals. Typically, these bacteria reduce insoluble Fe^{3+} found in protective metal coatings and in water treatment processes, into soluble Fe^{2+}. During this process the protective coating of ferric oxideis damaged, exposing the metal to the open environment (Javaherdashti, 2018). Fe^{3+} is also added to the water during treatment in the form of ferric chloride due to its success as a flocculant, coagulant, and odor neutralizer. Currently in America, over "80% of all ferric chloride is sold in municipal bids, for

municipal wastewater applications and potable water treatment applications" (HIS Markit, 2019).

2.4 *Legionella pneumophila*

Legionella bacteria are found in almost all potable and non-potable aquatic environments whether natural or man-made. They are gram-negative, non-spore forming, pleomorphic, bacteria that can grow in temperatures ranging from 20 to 40 degrees Celsius. *Legionella* are frequently found in biofilms and eukaryotic hosts, including protozoa, as well as, amoeba, to replicate in unfavorable conditions.

Approximately, 10,000 to 18,000 individuals are infected by *Legionella* each year in the United States, alone (Legionella Bacteria, 2020). Those who are immunocompromised are at the greatest risk of developing a deadly pneumonia, Pontiac Fever, or Legionnaire's Disease from *Legionella pneumophila*.

Legionella pneumophila is easily aerosolized which poses a great threat to the general public as it is often misdiagnosed as the common flu or cold and is found in almost any moist environment as shown in figure 2 below. A 2002 study found that survivors of Legionnaire's disease suffer long term effects where 66% had chronic neurological ailments and 63% had persistent neuromuscular issues (Lettinga et al.). Furthermore, 75% of individuals who survived Legionnaire's disease had prolonged fatigue (Legionella Bacteria, 2020 and Lettinga 2002). Since the bacteria have flagella, they are highly motile and can even be aerosolized, making the bacterium an even larger threat to public health.

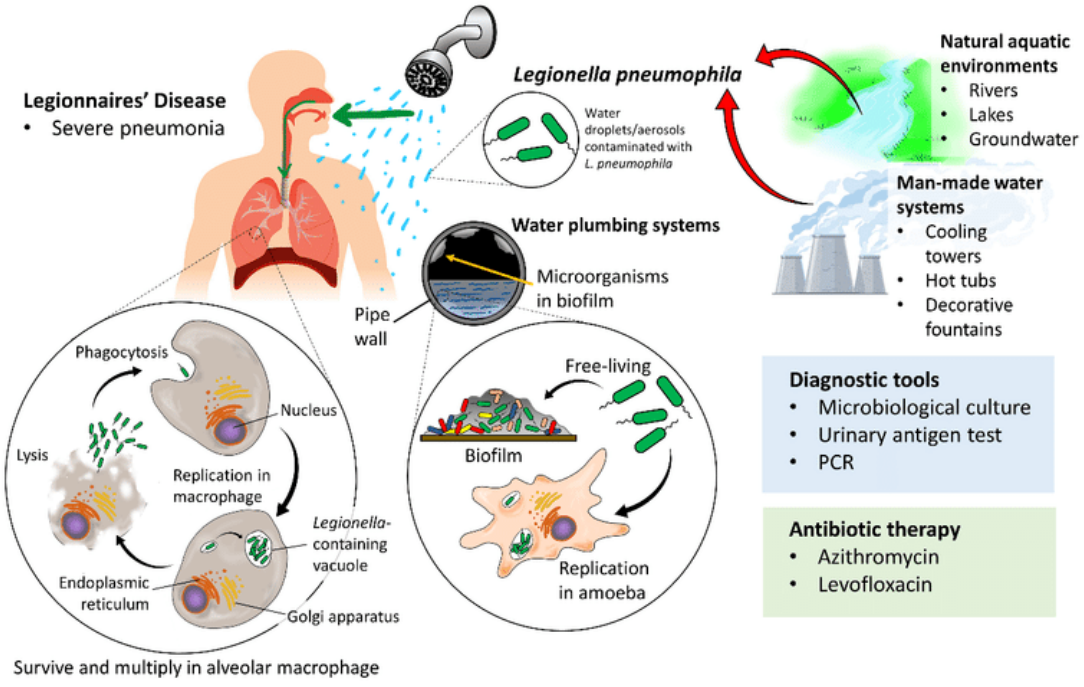

Figure 2. The life cycle, sources, and transmission of *Legionella pneumophila* (Ming, 2021).

2.5 *Mycobacterium*

Mycobacterium are a genus consisting of aerobic bacilli that are naturally found in water as well as soil and are the cause of several diseases. In humans, *Mycobacterium tuberculosis* and *Mycobacterium leprae* are responsible for tuberculosis and leprosy, respectively. Moreover, non-tuberculosis *Mycobacterium* that frequently infect immunocompromised individuals can cause life-threatening illness. The two bacteria responsible are *Mycobacterium avium* and *Mycobacterium intracellulare* which are often revered to as Mycobacterium Avium Complex (MAC). MAC is the most common cause of non-tuberculosis mycobacterial lung disease, today.

CHAPTER 3: MATERIALS AND METHODS

3.1 Bioreactors

The five bioreactors used in this project were made using 24in x 19in x 12in (60.96cm x 48.26cm x 30.48cm) plastic containers to house the various select coupons. It was ensured that a consistent flow of water along with water bacteria are maintained throughout this study. Thus, allowing for microorganisms to grow and develop biofilms as coupons are corroded. This setup was an effort to understand the microbial induced corrosion occurring at each test site. These bioreactors were green in color to prevent light penetration and had lids to avoid outside contamination as well as algae growth.

3.1.1 Design

The bioreactor was designed using 24in x 19in x 12in (60.96cm x 48.26cm x 30.48cm) green plastic with two plastic flaps for a lid. Each Bioreactor had four 8.5in x 11in x 5in (21.59cm x 27.94cm x 12.70cm) sampling boxes with eight partitions (Figure 3). Each partition was dedicated for one material type coupons, allowing each sampling box to independently house carbon steel, cast iron, copper, stainless steel 316 (SS316), stainless steel 304 (SS304), galvanized steel, chlorinated polyvinyl carbon (cPVC), and glass coupons. Each partition contained one type of each coupon with the exception of

galvanized steel which had two. This setup with various coupons contained inside of four boxes allowed for four separate collection dates. A plastic feed tube supplied fresh water to the top of the bioreactor while another tube on the other side allowed for water to flow out (Figure 3). This was done at a rate of 8 gallons per hour to reflect the average flow of wastewater, at 7.5 to 8 million gallons per day, experienced at Peoria's Butler Wastewater Reclamation Facility.

Figure 3**.** Bioreactor box at Arizona State University-Tempe lab with flow meter, water feed line and discharge line along with individual collection boxes housing various coupons identical to the field bioreactors.

3.1.2 Locations

There was a total of five bioreactor locations. The field sample location is a Butler wastewater reclamation facility located in southern Peoria, Arizona and Vistancia Production Well. The Butler Water Reclamation facility had three bioreactors, each at

pre-disinfection, post-UV and post-chlorination. The first bioreactor collected water at a pre-disinfection phase where the water had been pre-filtered to remove viruses. The second bioreactor location contained water that was treated using ultraviolet radiation. The third bioreactor was feed water that had undergone filtration, UV disinfection and chlorination. A fourth bioreactor was placed at a Vistancia production well located at Jomax Road and El Mirage Road in Peoria, AZ. The last bioreactor, used as a control, was placed in the Environmental Microbiology Laboratory at ASU and fed using premise plumbing water from the City of Tempe in Arizona.

3.1.3 Water Quality

The City of Tempe receives its drinking water from the Salt River Project Canal which receives its water from multiple surface water sources including the Salt River, Verde River, and Colorado River watersheds (City of Tempe, AZ, 2020). According to the City of Tempe, the annual reported range of chlorine is 0.08-1.10 ppm, as seen in Table 1 (2020). Water pH and hardness varies from 6.4-7.9 and 162-490 ppm, respectively (City of Tempe, AZ, 2020).

The Salt River Project along with the Central Arizona Project canal and reclaimed water are the main source of water for the City of Peoria. Table 1 shows the water has a higher pH, but lower hardness values with a range of 7.25-8.15 ppm and 68-290 ppm, respectively (City of Peoria, AZ, 2020). The range of chlorine is also higher than the City of Tempe at a range of 0.2-1.97 ppm.

Table 1. Drinking water quality characteristics reported in 2019 to the State of Arizona provided by the City of Tempe and City of Peoria.

Analyte	Units	Peoria	Valencia	Tempe
Alkalinity (avg.)	ppm	131	N/A	161
Hardness (avg.)	ppm	171	257	245
pH (avg.)	pH units	7.6	N/A	7.3
Turbidity	NTU	0.18	N/A	0.10
Chlorine (range)	ppm	0.2 - 1.97	0.63 - 1.17	0.08 - 1.10
Copper- 90th percentile result (year)	ppm	0.266 (2019)	0.18 (2018)	0.19 (2019)
Iron (range)	ppm			ND - 0.95
Sulfate (range)	ppm			53 - 200
Total Dissolved Solids (range)	ppm			350 - 1400
Total Organic Carbon (range)	ppm			0.92 – 3.1
Temperature (range)	□F			52 - 94

Source: (www.peoriaaz.gov/government/departments/water-services/water-resources and www.tempe.gov/government/municipal-utilities/water/water-quality/general-water-quality-information)

3.2 Coupons and Surface Area

Coupons of eight different materials were used in this experiment. They include carbon steel, cast iron, copper, stainless steel 316 (SS316), stainless steel 304 (SS304),

galvanized steel, chlorinated polyvinyl carbon (cPVC), and glass. Since coupons were of various shapes, using geometry, the surface area (SA) of each coupon was calculated by using the flowing equations:

SA of a Cylindrical Prism:$2\pi r^2 + 2\pi rh$

SA of a Rectangular Prism: $2(wl + lh + hw)$

SA of a Hexagonal Prism: $6ah + 3\sqrt{3}a^2$

Each of the coupons used one or more of the SA equations. The stainless-steel 316, 304 and galvanized steel coupons required SA of a hexagonal prism minus the SA of a cylinder. To estimate the SA of the galvanized steel the calculated surface area was multiplied by two to account for the two coupons used in an effort to achieve similar SA to the other coupons. The SA of a rectangular prism was used minus the SA of two cylinders was used for the copper coupons while to determine SA for cPVC the outer minus the inner SA of a cylindrical prism was used. Carbon steel and glass coupons were calculated by using the rectangular prism equations. The SA of the iron coupons were determined by using any combination depending on the shape of the coupon as seen in Figure 4 below. If the coupon was hexagonal then the SA of a hexagon minus the SA of a cylinder was used. In the event the coupon was irregular shaped pipe fitting then the coupon SA was determined by visually dividing the coupon in half then using the outer minus the inner SA of a cylinder for both sides (figure 4).

Figure 4. Different shapes of cast iron coupons used in this experiment.

3.3 Collection and Processing

Starting from the date sample boxes with coupons were placed in their respective bioreactors, one sample box was removed from the bioreactor at each site after one, three, six-, and 12-months incubation. After the samples were collected from Butler Wastewater Reclamation Facility, they were transported to Environmental Microbiology Laboratory at ASU within 45 minutes where a sample box was recovered from the lab bioreactor.

Different coupons from different sites were processed within six hours and plated for heterotrophic plate count using the process shown in figure 5. Briefly, using sterile forceps each coupon was individually placed in sterile petri dishes and 10 mL of sterile 0.5M PBS solution with 80 Tween (0.001%) was added to each plate. Using a flame sterilized wire brush the coupons were brushed to remove the biofilm then rinsed with another 10 mL of PBS solution. Half of the glass slides were processed using a straight edge sterile razor blade then set aside for microscope analysis. The total volume, 20mL, of PBS solution in each plate was then split between two sterile labeled, conical tubes. One set of the tubes was immediately stored at -80□C freezer while the other was stored at 4□C.

Figure 5. The processing of coupons from bioreactor boxes to Petri plates where they were scrubbed with PBS buffer and placed into conical tubes for plating or freezer storage.

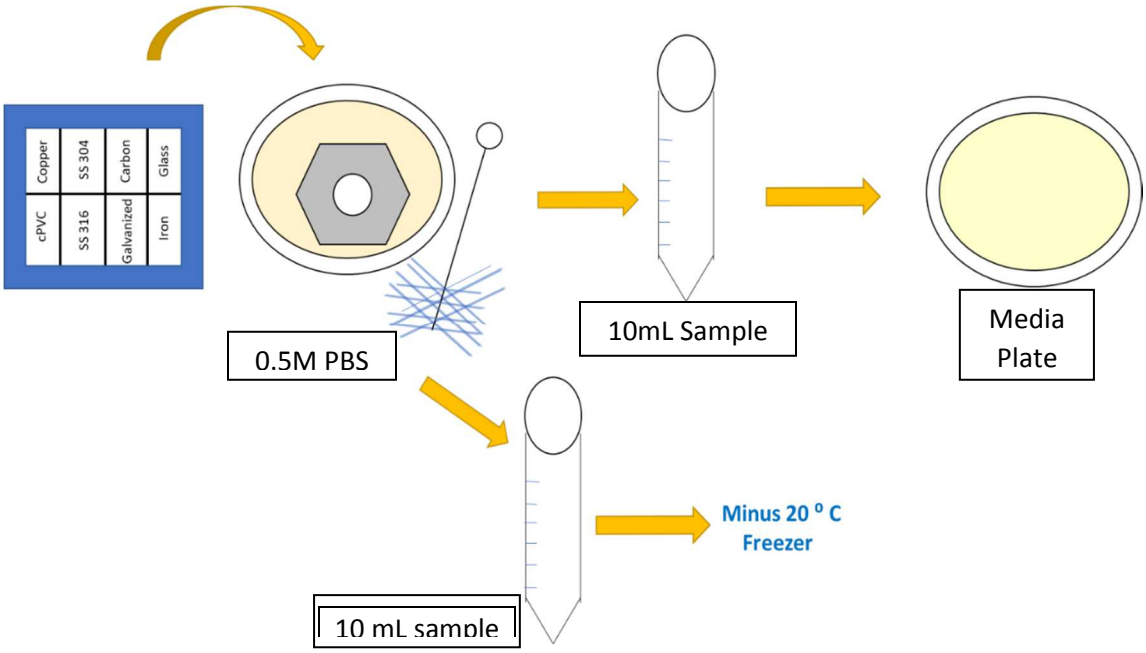

Using a Quick-DNA™ Fecal/Soil Microbe MiniPrep Kit (Zymo Research Cat. No. D6010) the sample elutes from cPVC, copper, and SS316 coupon biofilm DNA was extracted within 24 hours of sample collection. The samples were stored in sterile 1.5 mL Eppendorf tubes in a -80□C freezer for PCR analysis at a later date.

3.4 Media and Sparging

This experiment used several media types with samples that were collected and processed within 8 hours. The media was prepared in Environmental Microbiology Laboratory at ASU according to the specified directions and autoclaved at 121□C for 15 minutes. The only exception was Buffered Charcoal Yeast Extract, which was purchased as ready to use plates. The broth media for SRB was prepared using research grade

chemicals. The prepared broth dispensed in assay bottles was sparged with nitrogen gas to create anaerobic conditions. All media was stored at 4□C. Middlebrook Agar and BYCE plates were stored at 4□C and protected from light.

3.4.1 Heterotrophic Plate Count

BD Difco™ R2A Agar (REF 218263) was used for heterotrophic plate count for each sample. The media was properly cooled in a 48□C water bath for one hour then using the pour plate method. Briefly, 1.0 mL of biofilm sample was aseptically added sterile petri dish (100 x 15mm) followed by addition of to 13 mL of media tempered to 48 C. The plate was then gently swirled to mix the sample with liquified media. Assay plates were allowed to sit on work bench until the media was completely solidified. Plates were incubated inverted (placed with media side up), in a 22□C incubator for one week. Visible colonies were counted using a New Brunswick Scientific Colony Counter then recorded.

3.4.2 *Mycobacterium*

Middlebrook 7H10 Agar Base (Sigma-Aldrich SKU M0303) media along with Middlebrook OADC Growth Supplement (SKU MO678) were used for the detection of *Mycobacterium* using only the cPVC coupons from each sample collection. The agar was made following the directions provided on the media container then sterilized in the autoclave. The media was then placed in a 48□C water bath for 1 hour before the

appropriate amount of growth supplement was aseptically added using a pipet with sterile tips. Middlebrook 7H10 Agar plates were prepared by aseptically adding, 15.0 mL of the media solution to a 100 x 15mm sterile petri plate and let to solidify.

While the plates were solidifying each cPVC sample was processed for analysis. Briefly, 1.0 mL of each cPVC biofilm sample was aseptically transferred in to individually labeled 15 mL conical tube along with 0.5 mL of 3% HCl for 30 minutes. Next, 0.5 mL of 4% NaOH was added to each tube to neutralize the acid. 100 µL of each sample were then plated using the spread plate method. The plates were labeled, inverted, and placed in the dark at 37□C for two weeks before colonies were counted.

Suspected colonies of *Mycobacterium* were aseptically picked off the plate then placed in a sterile 1.5mL capped tube with 1.0mL of 0.5M PBS buffer. The tubes were then placed in a thermal cycler for incubation using the following programed specifications:

Total Volume	100 µL
Lid Temperature	105.0 □ C
Tube Temperature	97.0 □ C
Duration	15 minutes

Once the cycle was completed the samples were placed in the -80□C freezer for further analysis at a later date.

3.4.3 *Legionella*

Ready to use BYCE with VPC (Hardy Diagnostics REF W79) were purchased for the detection of *Legionella*. Each cPVC coupon collected was processed for analysis as follows. Briefly, 1.0mL of the samples were aseptically transferred into sterile, 15mL conical tubes along with 1.0mL of 0.2M HCl. Next, the samples were incubated at room temperature for 30 minutes. After incubation, 100 µL of each biofilm sample was aseptically plated using the spread plate method. The plates were incubated in the inverted position (media side up) at 37□C for up to 10 days inside of a closed plastic bag. Colony counts were recorded, and each plate was placed under UV light to determine if any colonies fluoresced to suggest they were *Legionella*. Samples were also aseptically collected off the plates and stored in a 1.5mL capped microfuge tube with 1.0mL of 0.5M PBS buffer at -80□C for further testing.

3.4.4 Sulfur Reducing Bacteria

The liquid media (broth) for culturing SRB was prepared in the lab. The media required preparation of four independent solutions to prevent the formation of precipitates. Solutions one contained; 2.0g $MgSO_4$, 5.0g Sodium Citrate, 1.0g NH_4Cl, and 300mL of nano pure water. Solution two was comprised of 1.0g $CaSO_4$ X $2H_2O$ in 100mL of nano pure water. Solution three contained 0.5g K_2HPO_4 in 200mL of nano pure water. Lastly, Solution four contained 3.5g Sodium Lactate, 1.0g Yeast Extract, and 400mL of nano pure water. The pH of each solution was adjusted to 7.5 before being autoclaved. Once autoclaved all solutions were aseptically mixed, cooled, then stored at 4□C.

Using a sterile 21-gauge syringe, 10mL of SRB media was injected into a sterile, vacuum sealed vial with a rubber self-sealing lid. Next, 1.0mL of water from each sampling site bioreactor bin was injected using a 27-gauge sterile syringe. Each labeled vial was then sparged nitrogen gas using 21-gauge needles and then placed at 37□C for 72 hours (Figure 6). Samples showing signs of turbidity had 200 µL of sample removed using a sterile syringe then placed in labeled PCR tubes. The samples were then processed in a thermo-cycler for 15 minutes at 97□C. Lastly, they were stored at -80□C for PCR.

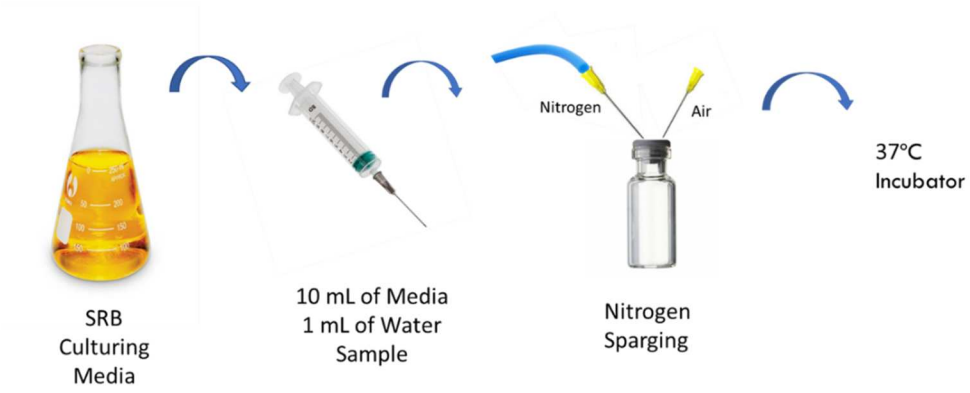

Figure 6. SRB testing and sparging process used in this experiment.

3.5 Microscopy

Microscopic observations of all the glass slide coupons were performed for every sample collection. The slides were sequentially stained with vital dyes to monitor biofilm development and various bacterial types present. Once half the glass slide was processed for media plating, it was placed in Cosmine solution for one minute then rinsed with deionized (DI) water for 30 seconds. Next, it was placed in Potassium Chromate solution

for one minute before air drying. After the slide was dry it was inspected under an Olympus BX60 microscope. Once images were taken the slide was rinsed for 30 seconds with DI water then placed in Crystal Violet solution for 30 seconds. The side was then rinsed for one minute using DI water before air dried and placed under the microscope for more images (Figure 7).

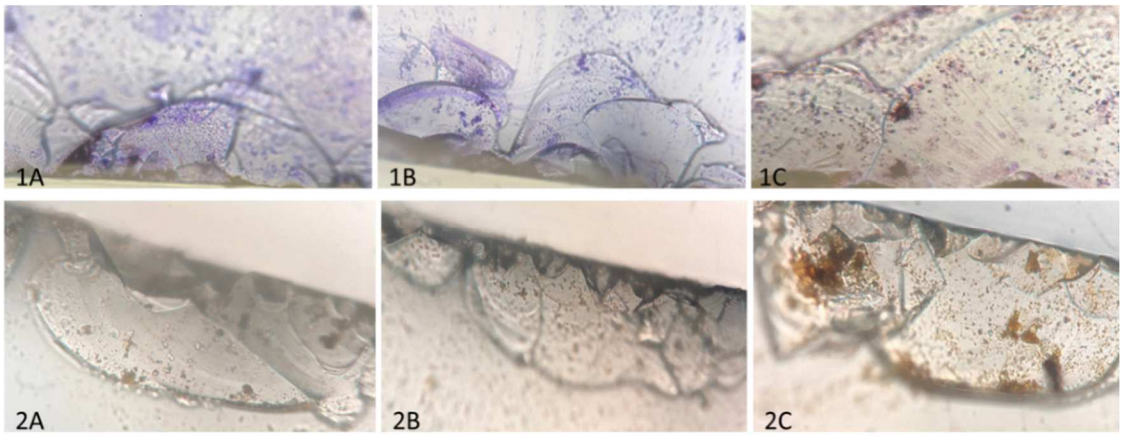

Figure 7. Microscopy images of glass coupons from the post-UV bioreactor bins where A, B, and C are the month of October (2020), December (2020), and March (2021), respectively. Row one shows Cosmine and Potassium Chromate staining. Row 2 shows Crystal Violet stain.

3.6 Polymerase Chain Reaction

Samples from selective media plates were analyzed by Quantitative Polymerase Chain Reaction (qPCR) to verify the presence of *Mycobacterium, Legionella* and sulfur reducing bacterium *D. vulgaris.* The universal primers were designed then purchased through Integrated DNA Technologies. The first set designed is for testing the biofilm DNA and the second set for colonies isolated using SRB, BYCE, and Middlebrook medias. The first set for biofilm DNA is 54 base pairs long while the other is 19 base pairs (Table 2).

Table 2: Primers and sequences designed for biofilm DNA and isolated colonies.

Primer	Sequence (5' to 3')
Biofilm-Forward	TCG TCG GCA GCG TCA GAT GTG TAT AAG AGA CAG GTG YCA GCM GCC GCG GTA A
Biofilm-Reverse	GTC TCG TGG GCT CGG AGA TGT GTA TAA GAG ACA GGG ACT ACN VGG GTW TCT ATT
Colony-Forward	GTG YCA GCM GCC GCG GTA A
Colony-Reverse	GGA CTA CNV GGG TWT CTA AT

CHAPTER 4: RESULTS AND DISCUSSION

MIC of each material type varies depending on the coupon material as well as the water quality (pre or post treatment) and the incubation period. The corrosion was evident based on visual observation and biofilm formation on the coupons. Due to the heavy corrosion rates on some of the coupons, heterotrophic bacteria (HPC) were enumerated. Over the duration of the year, biofilm bacterial concentration increased suggesting higher corrosion rates.

4.1 Visual Coupon Observation

Over the course of the year, the overall visual corrosion increased for the majority of the coupons at each of the sampling locations within the reclamation facility. There were minor fluctuations in the average concentration of bacteria in the biofilms for each of the same coupon materials depending on the sampling location. In general, iron and carbon steel displayed the highest whereas, SS304 and SS316 displayed the lowest visual corrosion rates.

The average number of CFU per cm^2 for the coupons varied for each coupon at every sampling point. Data suggests that stainless steel and galvanized steel have the

highest corrosion rates whereas copper has the lowest corrosion rates, regardless of seasonality.

Copper displayed limited visual corrosion after one year. The coupons became increasingly more tarnished each time the samples were collected and visually did not fluctuate depending on the seasonal changes. Vistancia Production Well showed the most visible corrosion with the presence of turquoise deposits on the surface of the coupon which is indicative of Copper (II) Chloride (figure 8). This is likely due largely to the presence of chlorine ions reacting with the copper.

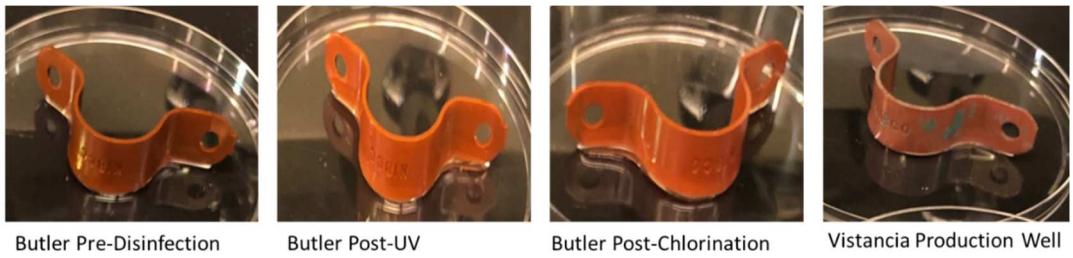

Figure 8. MIC on field copper coupons after one year

The cPVC coupons appear to be visually unaffected by MIC after one year (Figure 9). All collected samples, appear to have no cracks, rot, or lose surface integrity. The surface remained smooth, and the color did not change.

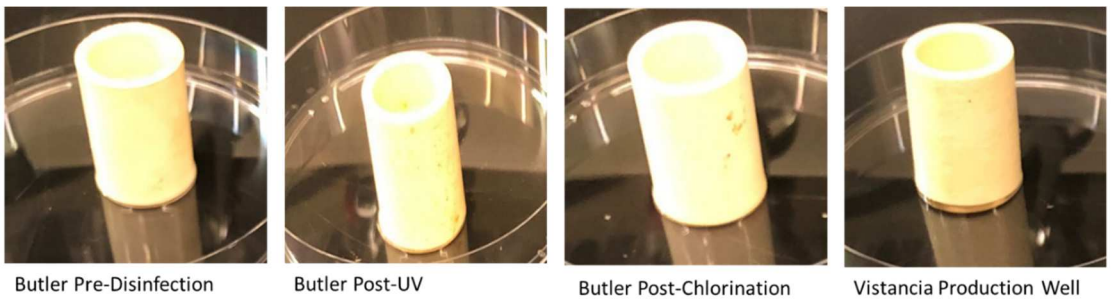

Figure 9. MIC on field cPVC coupons after one year

Galvanized steel showed visual signs of corrosion at each of the field sampling sights after one year. The corrosion present at Butler Wastewater Reclamation Facility is

present in a brownish-red rust color whereas Vistancia corrosion is more of a white deposit. This is likely because the brownish red is iron oxide while the white deposits seen at Vistancia is damage done to the protective zinc coating on the galvanized steel that presents itself in the form of ZnS (Figure 10).

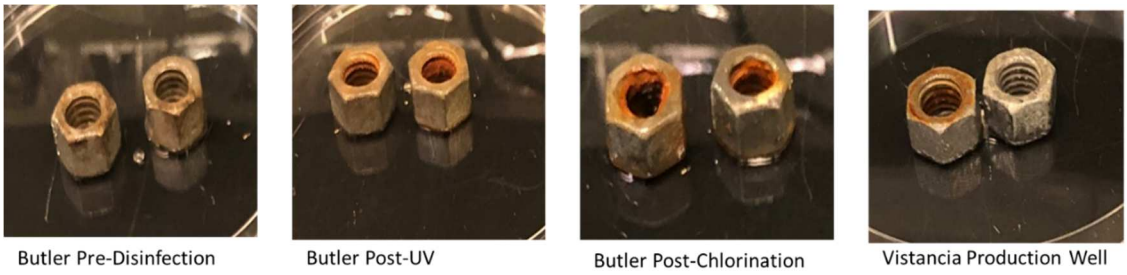

Figure 10. MIC on field galvanized steel coupons after one year

Carbon steel had one of the most rapid visual corrosion rates seen in the field samples. All samples from Butler were heavy with rust and flaked off. The coupons suffered extensive damage after one year and showed signs of cracking corrosion (Figure 11). Carbon steel from Vistancia showed corrosion as white mineral deposits leaching form the metal as much as it did brownish red.

Figure 11. MIC on field carbon steel coupons after one year

The stainless steel 316 and 304 coupons showed no visual signs of corrosion after one year for any of the sampling locations (Figure 12 and Figure 13, respectively). All SS 316 and 304 coupons remained shinny and did not have any obvious signs of MIC to their protective coatings.

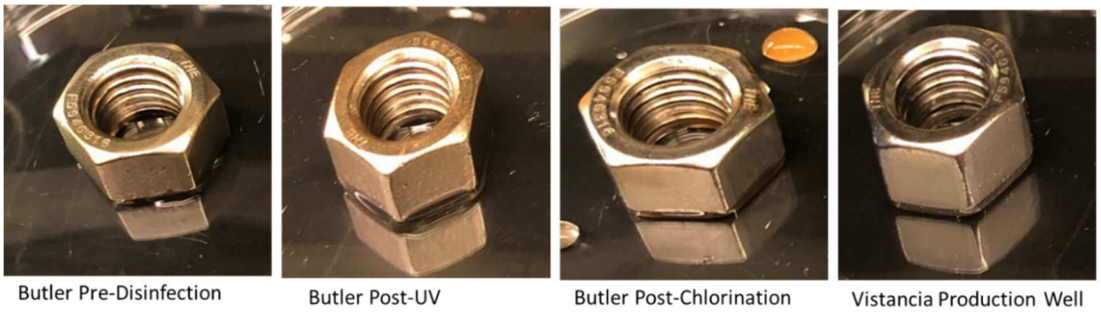

Figure 12. MIC on field SS316 coupons after one year

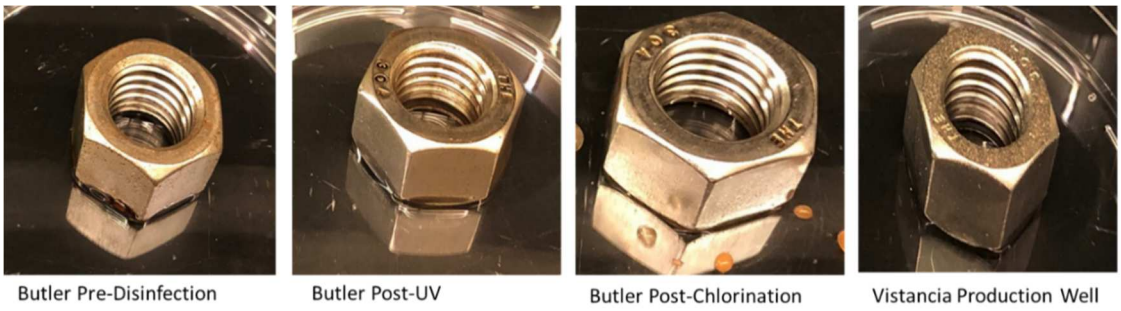

Figure 13. MIC on field SS304 coupons after one year

Cast Iron coupons had visual signs of rapid corrosion occurring that did not seem influenced by seasonality. The field samples after one year at the Butler location were covered in thick, brownish red rust. Some of the rust showed a black precipitate as seen at Butler's Post-UV sampling site (Figure 14). Vistancia also had signs of heavy corrosion in the form of brownish red rust, black precipitate, and white mineral deposits.

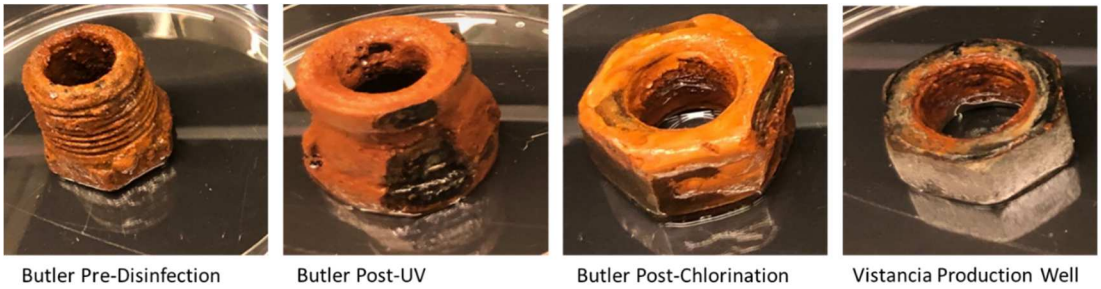

Figure 14. MIC on field cast iron coupons after one year

The glass control coupons did not change much during the experiment. Samples from Butler's pre-disinfection and post-UV were brown with sediments but did not

appear to have thick layers of rust or biofilm formation (Figure 15). This is expected since glass offers no source of carbon to be utilized by bacteria as a source of food. Therefore, any biofilm present on these coupons would be receiving nutrition from the media, not from corroding the material itself.

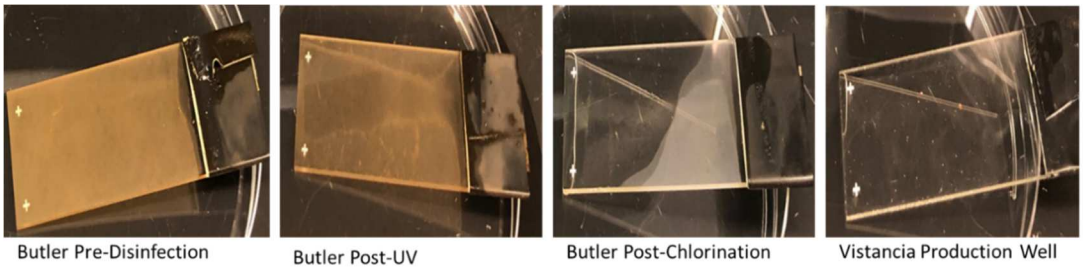

Figure 15. MIC on field glass control coupons after one year

4.2 Heterotrophic Plate Count

As expected, the glass control biofilm had some of the lowest colony counts followed by copper. Galvanized steel biofilms had some of the highest CFUs whereas cast iron and carbon steel coupon biofilms had an abundance of rust accumulated on the surface of the coupon that plating the biofilm was difficult due to the brown coloration that occurred when plating the samples.

The field samples for the copper coupon biofilm were varied in size but had similar colors for the Butler Reclamation Facility samples (Figure 16). The colonies were mostly white in color, round, and convex in shape. Amoeba grew on the pre-disinfection plate along with tiny white bacterial colonies and a few tan colored colonies appeared on the post-chlorination plate along with a fungus. The most colony growth occurred on the post-UV plate while the Vistancia Production Well HPC showed orange-brown colored colonies which may indicate the presence of *Thiobacillus*, but further DNA analysis is needed to confirm. The average concentration after one year was 1207 CFUs/cm^2.

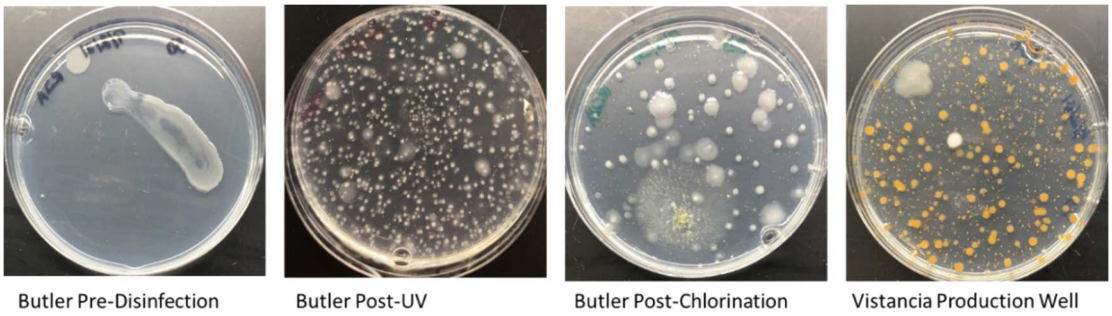

Figure 16. HPC growth from field copper coupon biofilm after one year

The HPC concentration for the field cPVC coupon biofilms were typically lower than the concentration for the steel coupon biofilms. This is highly expected since the majority of bacteria can utilize metals and organic carbons as a food source but not many are able to use the complex polymer chains that make up plastic. Furthermore, cPVC is made by chlorinating a polyvinyl chloride resin which gives it extra protection from microbial decay due to the strength of the carbon-chloride bond. However, the average CFU per cm^2 on the year old cPVC coupons was higher at an estimated 1957 CFUs/cm^2 compared to the copper coupons at 1207 CFUs/cm^2. This could be explained by biofilm formation on cPVC. While not all bacteria are able to colonize plastic, *Pseudomonas* is known to do so and is also known for its robust EPS production which can house other bacteria within the cPVC coupon biofilm. Furthermore, *Pseudomonas* can grow in low carbon-nitrogen ratio environments and is a common denitrifying bacteria found in wastewater treatment plants (Chen et al. 2022).

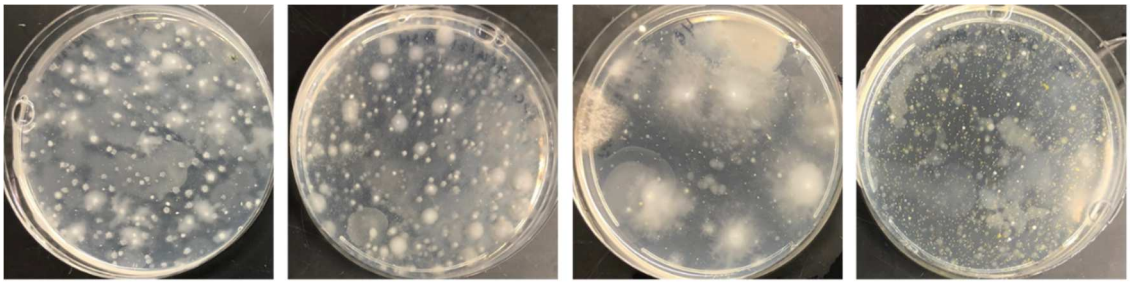

Figure 17. HPC growth from field cPVC coupon biofilms after one year

Galvanized steel coupons after one-year had extensive biofilm growth. The colonies were consistently smooth, round, and convex in appearance for this type of sample throughout the experiment (Figure 18). The post-chlorination and post-UV coupon biofilms had consistently lower concentration (CFUs/cm^2) compared to pre-disinfection and Vistancia. After one year the average CFU per cm^2 on galvanized steel was calculated to be 18663. This might be because UV and chlorine disinfection had effectively reduced the total number of microbes while at the same time resulting corrosion of the galvanized steel protective zinc coating. Thus, the natural disinfection process at the treatment facility allowed for easier access to the alloy by corrosive bacteria because the protective zinc coating is compromised and can no longer starve the bacteria of manganese to inactivate them with high concentrations of zinc (Porcheron, 2013). However, though zinc is toxic in high concentrations to bacteria, it is needed for cellular metabolism, gene expression, and DNA replication (Porcheron, 2013).

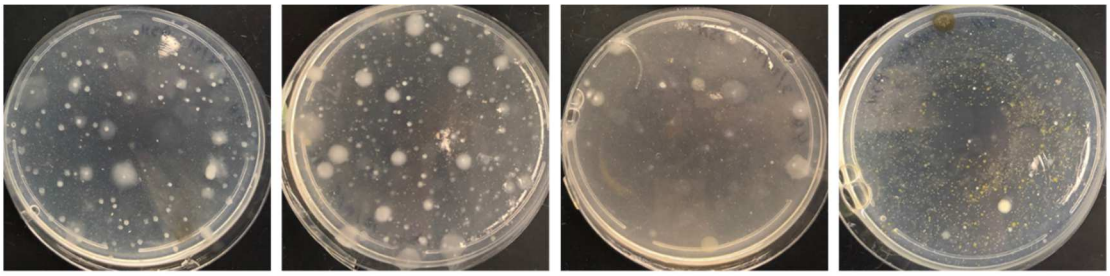

Figure 18. HPC growth from field galvanized steel coupon biofilms after one year

Carbon steel plates had a high amount of rust content and robust colony growth. This is common due to carbon steel having a higher carbon content compared to other steels. Naturally, the higher carbon content mixed with iron to make carbon steel an excellent choice for bacterial colonization. The colonies were mainly smooth, white, convex appearance and much smaller in size compared to colonies from other coupon types (Figure 19). This is likely because of the heavy corrosion, smaller colony size, and discoloration of the plates. The average visibly countable CFU per cm^2 on the carbon steel coupon biofilms was estimated to be 1699.

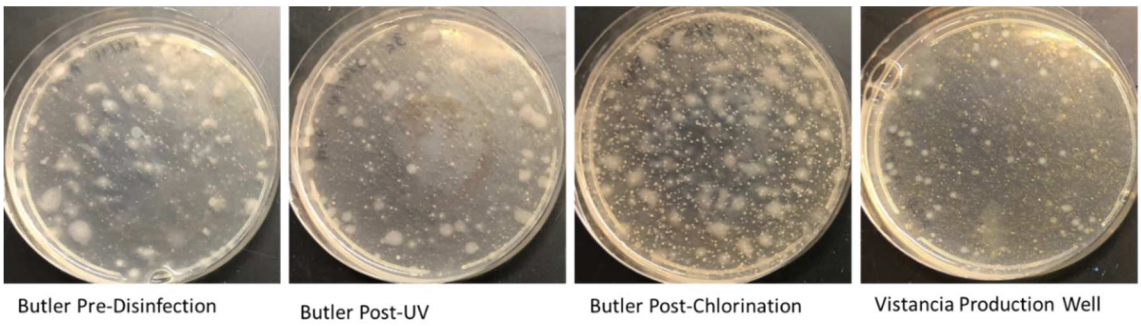

Figure 19. HPC growth from field carbon steel coupon biofilms after one year

Stainless steel 316 had the same typical smooth, white, convex bacterial colony growth on HPC from the coupon's biofilm bacteria. Some of the other bacteria embedded withing the agar was white as well with a few red colored colonies at the Butler

Reclamation Facility (Figure 20). Roughly half of Vistancia Production Well's coupon biofilm growth was a lemon-yellow color on HPC media. The overall calculated average CFU per cm^2 for SS316 was estimated to be 4069.

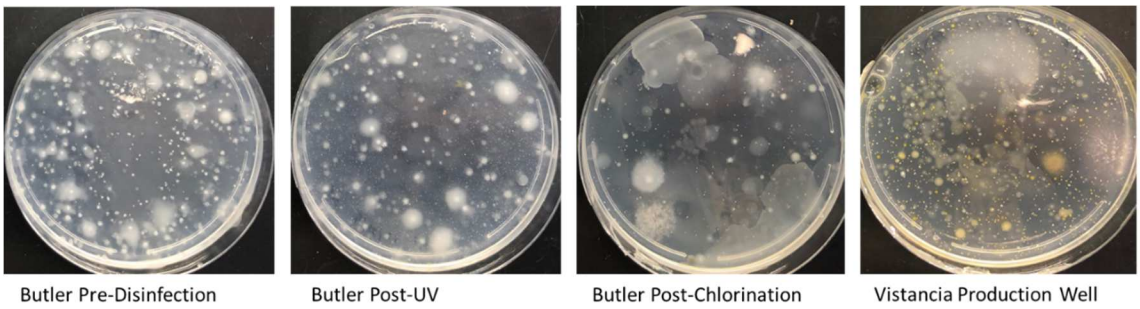

Figure 20. HPC growth from SS316 field coupon biofilms after one year

The bacteria which were found in the one-year SS304 biofilms were similar in appearance to the SS316. The bacterial colonies for the Butler Reclamation Facility were also mostly small, smooth, white, and convex in appearance (Figure 21). There were only a few red colored colonies and approximately half of the Vistancia Production Well CFUs were lemon-yellow in appearance as well. The colonies were slightly larger and more visible than SS316, but this could be due to fewer colony counts allowing for larger colony growth due to more resources available on the plate. The average CFU per cm^2 was calculated to be 2884 which is about three-fourths the amount of CFUs that appeared on the SS304 plates.

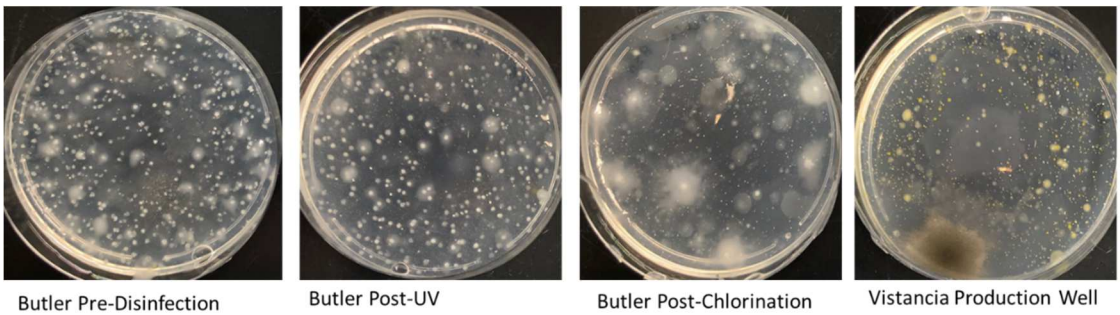

Figure 21. HPC growth from SS304 field coupon biofilms after one year

Cast iron coupons had the highest corrosion rates which polluted the HPC plates with rust. Thus, the CFUs were difficult to count and only the visually countable CFUs on the surface were considered. The countable average CFU per cm^2 in cast iron biofilm coupons was 2753. The plates with the most rust were the post-UV and post-chlorination plates from the Butler facility (Figure 22). This is due to the corrosion effect that water and chlorine both have on cast iron along with the bacteria's high affinity to iron. Furthermore, UV light reacts with iron to accelerate the corrosion rate.

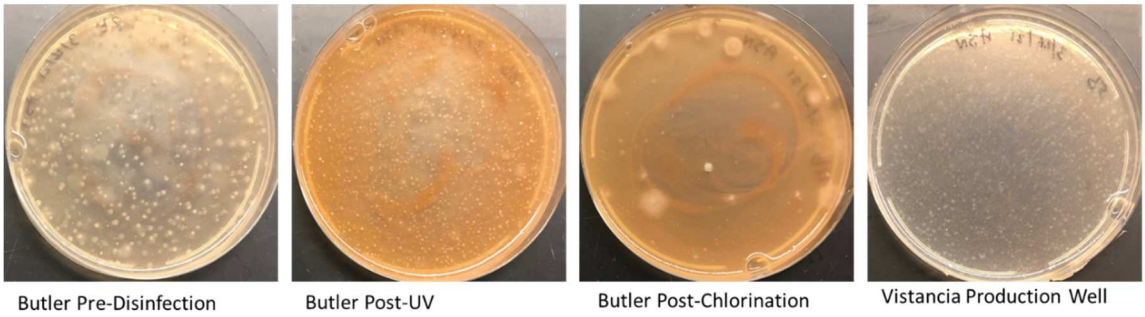

Figure 22. HPC growth from cast iron field coupon biofilms after one year

The glass control coupons had minimal HPC growth in comparison to the other coupons with an average CFU per cm^2 of 1994. The colonies were also similar in size with white coloring (Figure 23). The shape was circular with smooth edges and convex for the Butler field samples. However, the Vistancia control coupon had colorful growth on HPC (Figure 23). Some of the bacterial colonies were white while others were yellow or salmon pink in color. Due to Vistancia being an aquifer storage and recovery for groundwater recharge we would expect to see different bacteria found in the well compared to the microbes we see in the wastewater treatment facility.

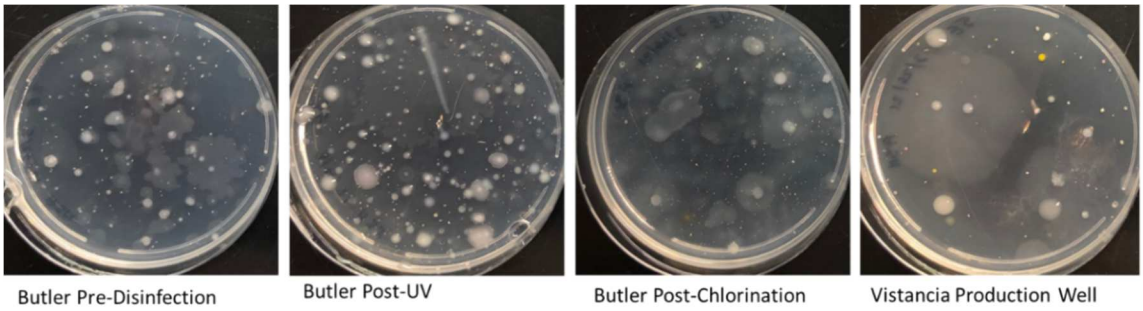

Figure 23. HPC growth from glass control field coupons at one year

The average CFU per cm^2 varies among the different coupon types and may depend on seasonality for some of the material types (Figure 24). The graph is based on visually countable CFUs which explain why iron and carbon steel are low when bacteria have a high affinity for iron. Galvanized steel shows some of the highest concentration along with SS316. The average CFU for the glass control drops significantly at the six-month marker. This may be explained by the seasonal changes since the six-month collection occurred in early March after the coldest part of the season and the three-month collection in December was before the coldest part of the season. Furthermore, glass offers no insulation and biofilms have difficulty establishing themselves on the smooth surface to protect the fragile bacteria within. Both cPVC and copper appear to remain unaffected by seasonal changes along with SS316 and SS304.

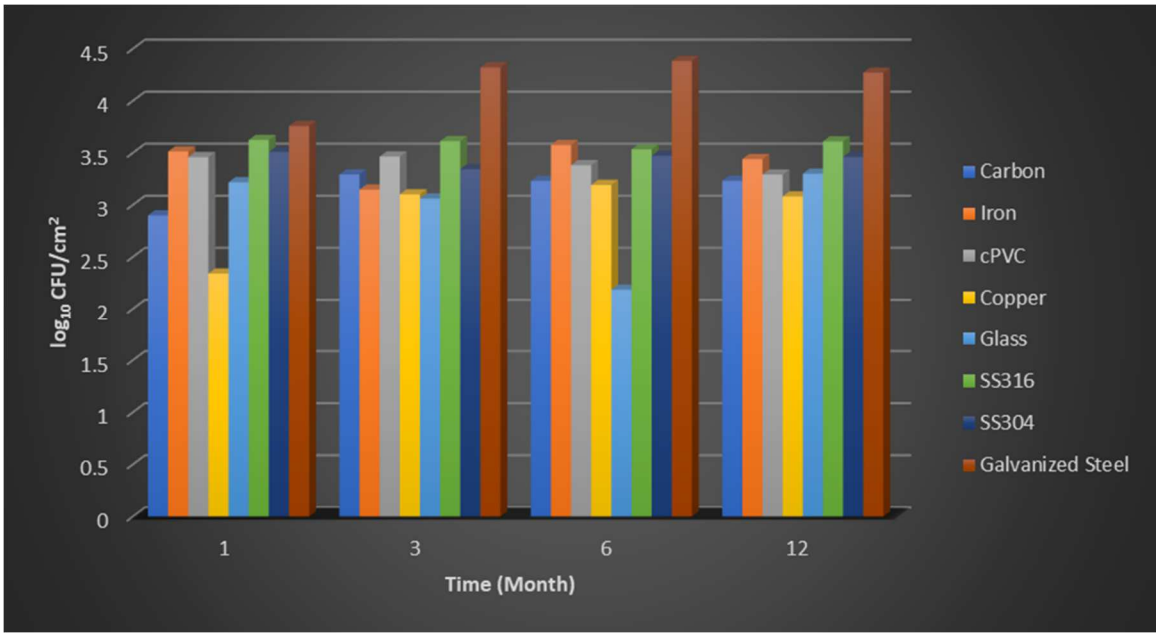

Figure 24. The average HPC for the various coupon types at all sampling locations for each sampling collection time

Upon closer examination of the SS316 and SS304 with galvanized steel, there is not much of a change in CFUs per cm^2 (Figure 25). SS316 and SS304 are nearly identical in comparison for each of the different seasonal collection times. Furthermore, there is only a 0.07 log difference between galvanized steel and SS316.

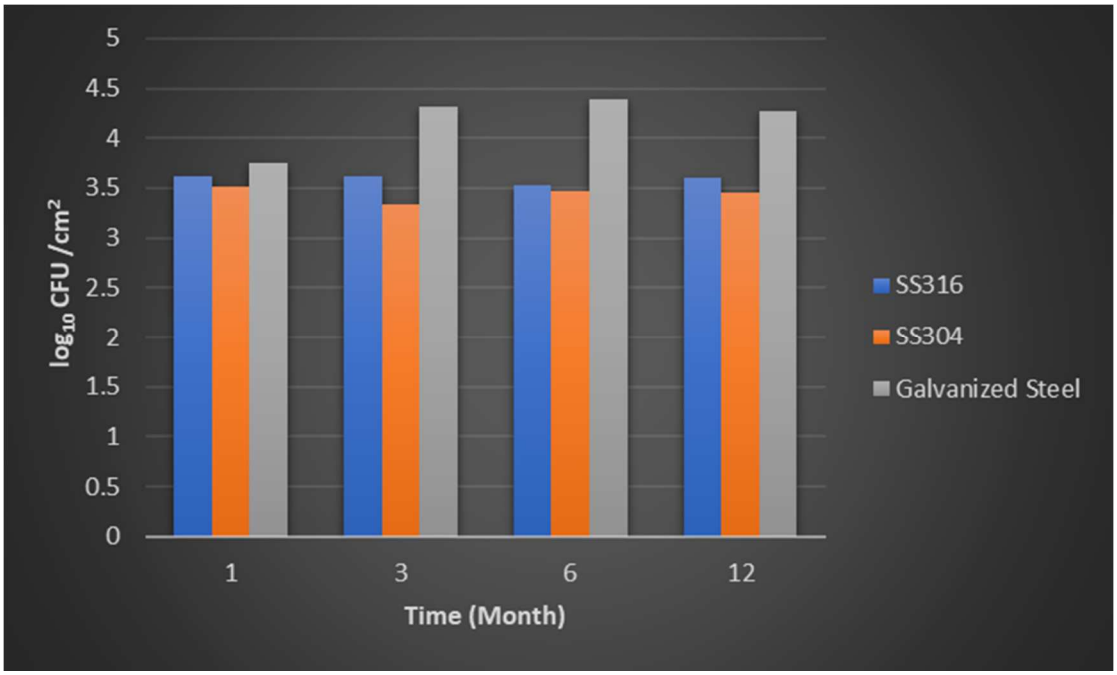

Figure 25. Average HPC for SS316, SS304, and galvanized steel for all sampling locations at each collection time

The highest concentration of HPC for carbon steel after one year was at the post-chlorination treatment train (Figure 26). This may be the result of bacteria that have survived the treatment process utilizing iron and carbon to grow and reproduce. Furthermore, accelerated corrosion rate was detected in carbon steel at post-UV causing more damage that allows biofilms to establish. Interestingly pre-disinfection and Vistancia have the same CFUs which may be explained because the raw wastewater has greater levels of nutrients and there is not much need for microbial degradation of the carbon steel. Vistancia receives treated water that has been chlorinated which would inhibit microbial growth. The ASU microbiology laboratory is expected to have the lowest colony counts since it is a treated water supply.

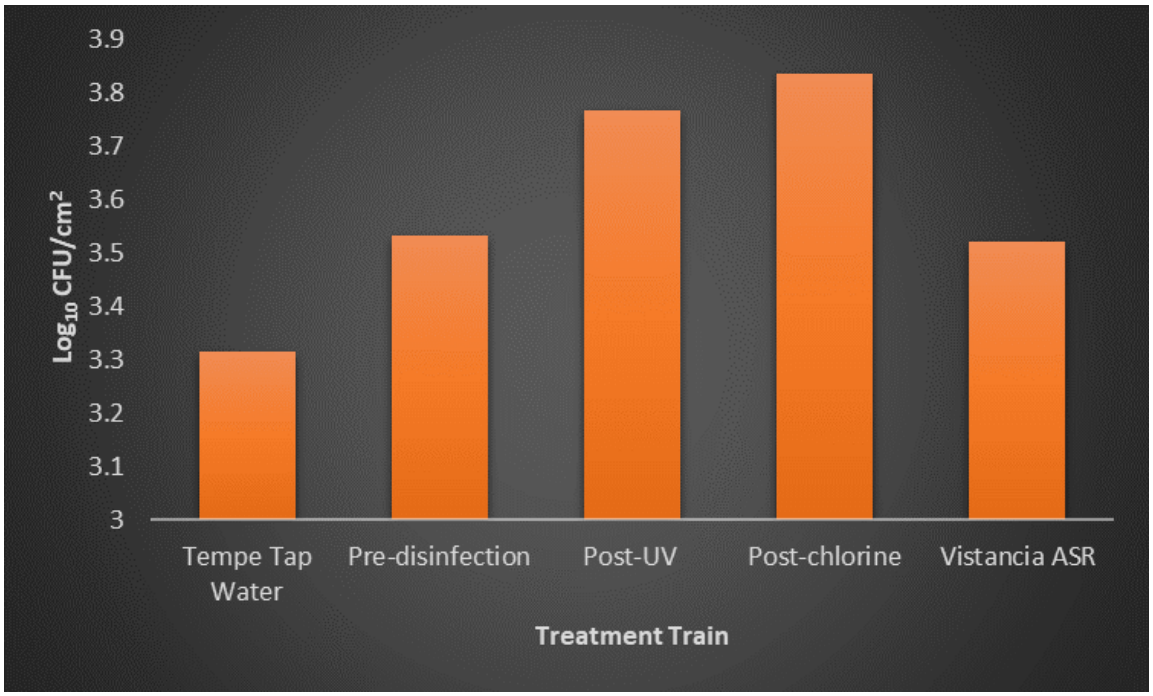

Figure 26. HPC concentration on carbon steel after one-year

The HPC concentration for cast iron was the lowest during the post-UV treatment train process (Figure 27). The post-UV had the densest amount of rust particles within the media, making colony counts difficult (Figure 22). Post-Chlorination HPC concentration are also low because of high corrosion. The cast iron coupons at ASU's microbiology laboratory and Pre-disinfection at the Butler plant have a similar HPC concentration which may be explained by bacteria containing siderophores. Siderophores help bacteria obtain iron and they have a high affinity for iron. Vistancia had the highest CFU concentration and can be explained because it is an aquifer storage and recovery site. Cast iron is made with graphite which easily breaks and is easily degraded in soil or wet environments. When combined with soil and water microbes, the brittle material allows for easy corrosion and bacterial colonization.

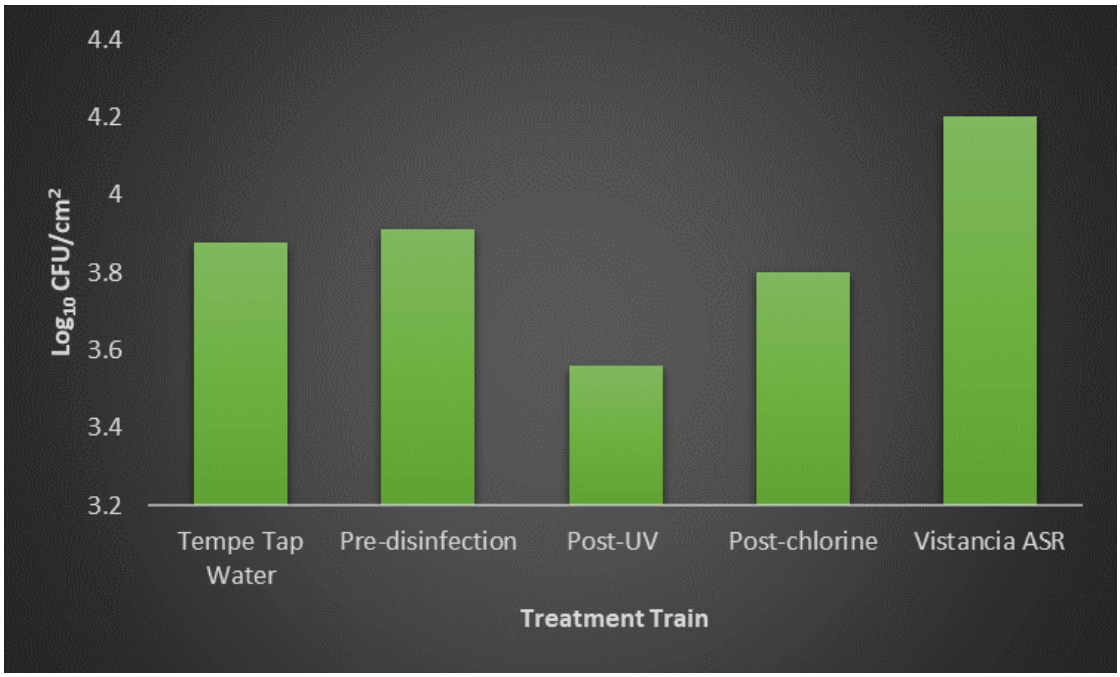

Figure 27. HPC concentration on cast iron after one-year

The overall HPC concentration on cPVC after one year was rather consistent throughout the treatment train process except for Vistancia (Figure 28). This is expected because cPVC is a plastic polymer which not many microorganisms can biodegrade.

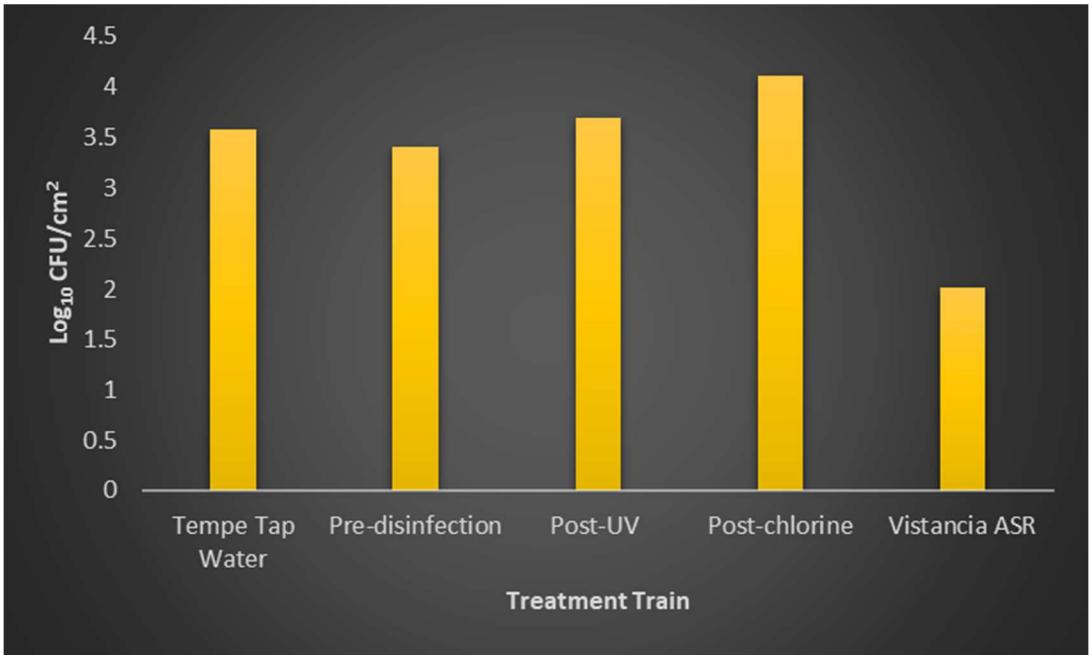

Figure 28. HPC concentration on cPVC after one-year

The HPC concentration for copper was the same throughout the treatment train except for Vistancia (Figure 29). This is expected considering that copper reacts with chorine, used as a disinfectant in the treatment train process, to form Copper (II) Chloride. This reaction exposes the surface of the material to allow for biofilm formation to occur. The significantly lower CFUs at Vistancia are likely the result of minimal chlorine residual present at the production well to react with the copper ions.

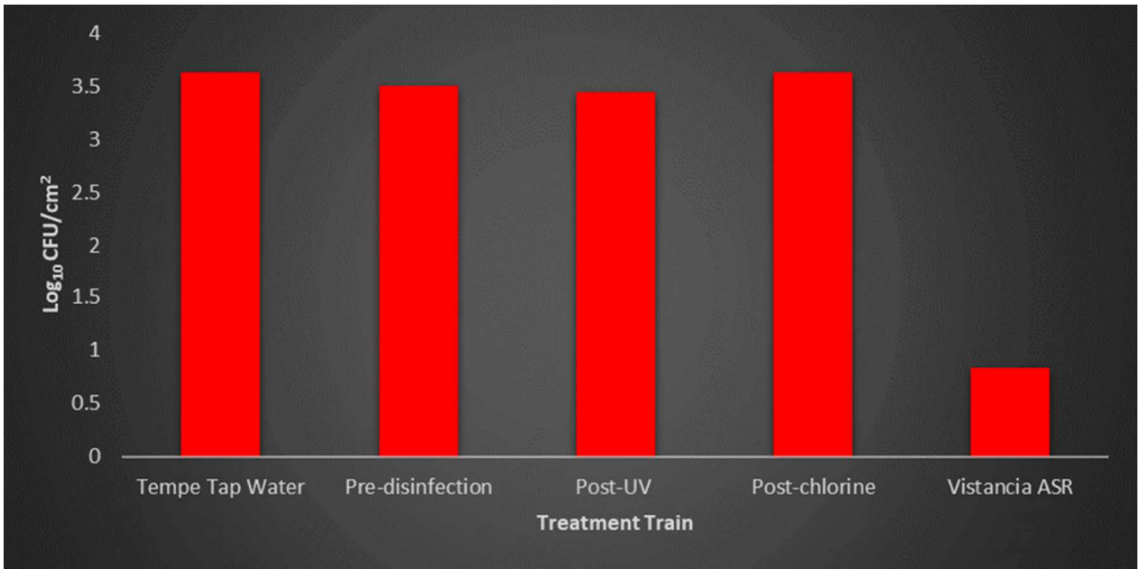

Figure 29. HPC concentration of copper after one-year

Glass had an unexpectedly high concentration of HPC (Figure 20). This can be explained by the concentration of organic matter that has accumulated on top of the material after one year. As the organic matter accumulates, biofilms can absorb the carbon within the biofilm for bacterial growth. Pre-disinfection had considerably lower HPC concentration. This was likely due to the glass coupon becoming dislodged from the plastic divider that suspended the coupon in the media. Since the glass coupon was at the bottom of the bioreactor sampling box, only one side of the coupon was easily accessible

for biofilm formation, thus hindering the colonization of the glass. The last sampling collection also occurred after summer. Since glass conducts heat, it is possible that the bacterial growth was inhibited by the heat, or the biofilm detached in transportation.

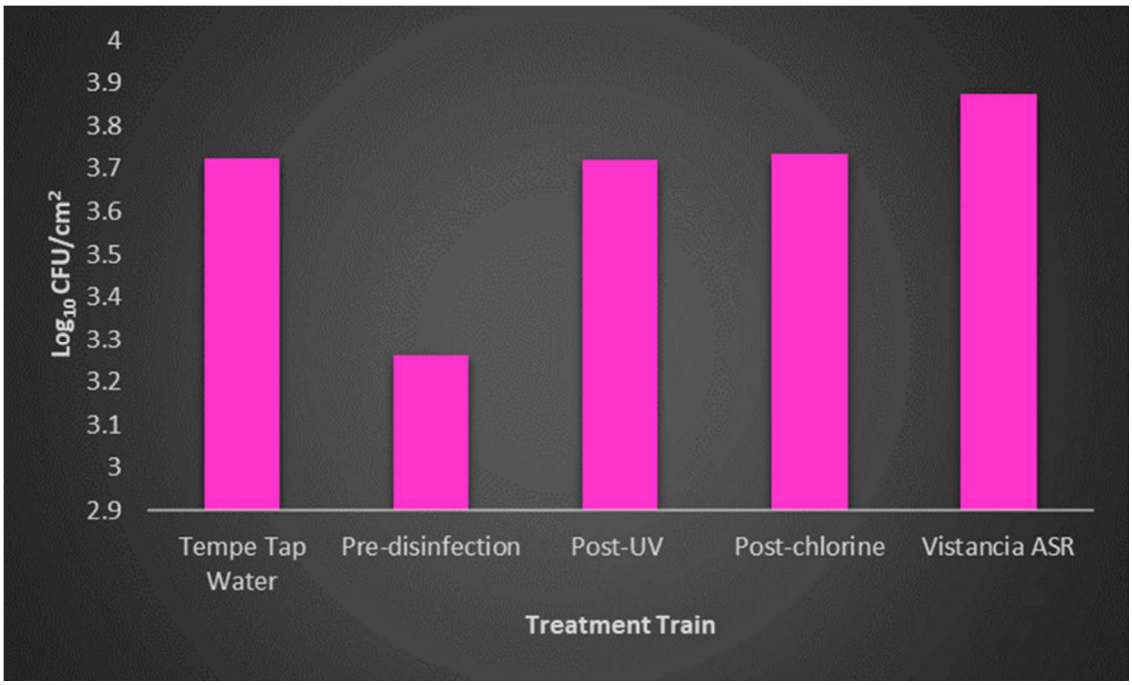

Figure 30. HPC concentration on glass after one-year

The concentration on SS316 is lowest for Vistancia (Figure 31). SS316 has molybdenum added to make the metal even stronger and more resistant to corrosion. Furthermore, due to the lack of residual chlorine, which reacts with stainless steel, damaging the protective coating and exposing the metal directly to microorganisms for easy colonization. Since chlorine residual is present in tap water and wastewater, it is expected that the corrosion of stainless steel would be higher due to chemical, salt, and microbial factors.

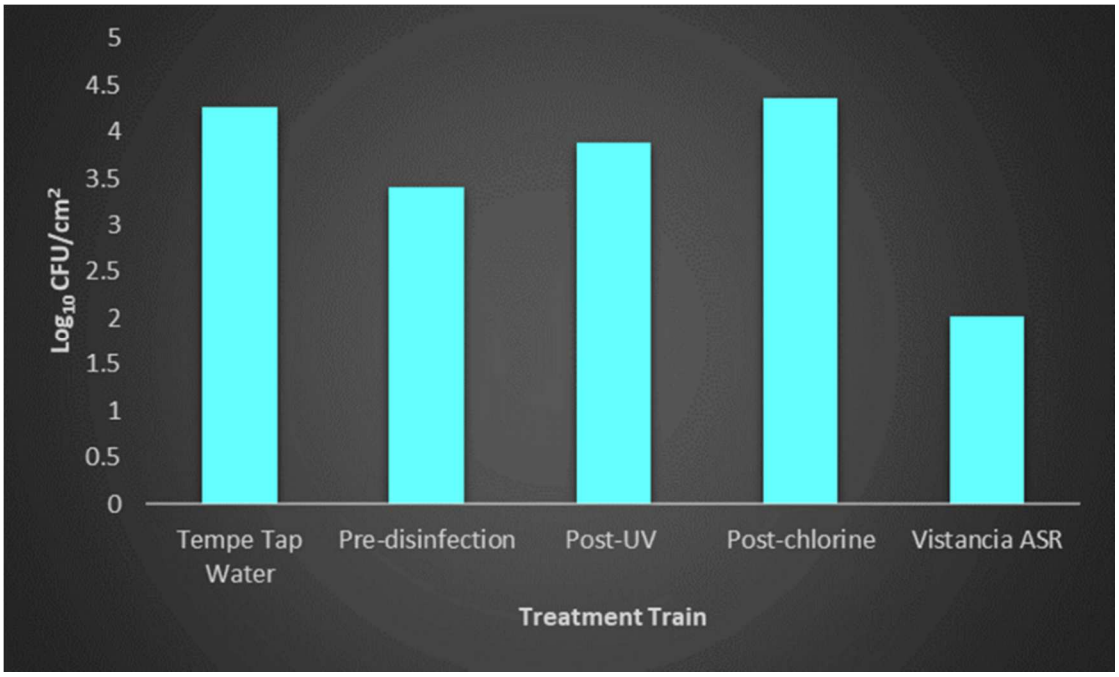

Figure 31. HPC concentration on SS316 after one-year

The HPC concentration on SS304 after one-year is consistent throughout the treatment train process (Figure 32). SS304, much like SS316, is very susceptible to damage by chlorine which explains the HPC concentration for ASU's microbiology lab and the Butler facility. The high HPC concentration at Vistancia is likely due to chemicals or a high salt concentration in the production well which rapidly damages the protective coating of SS304 compared to SS316.

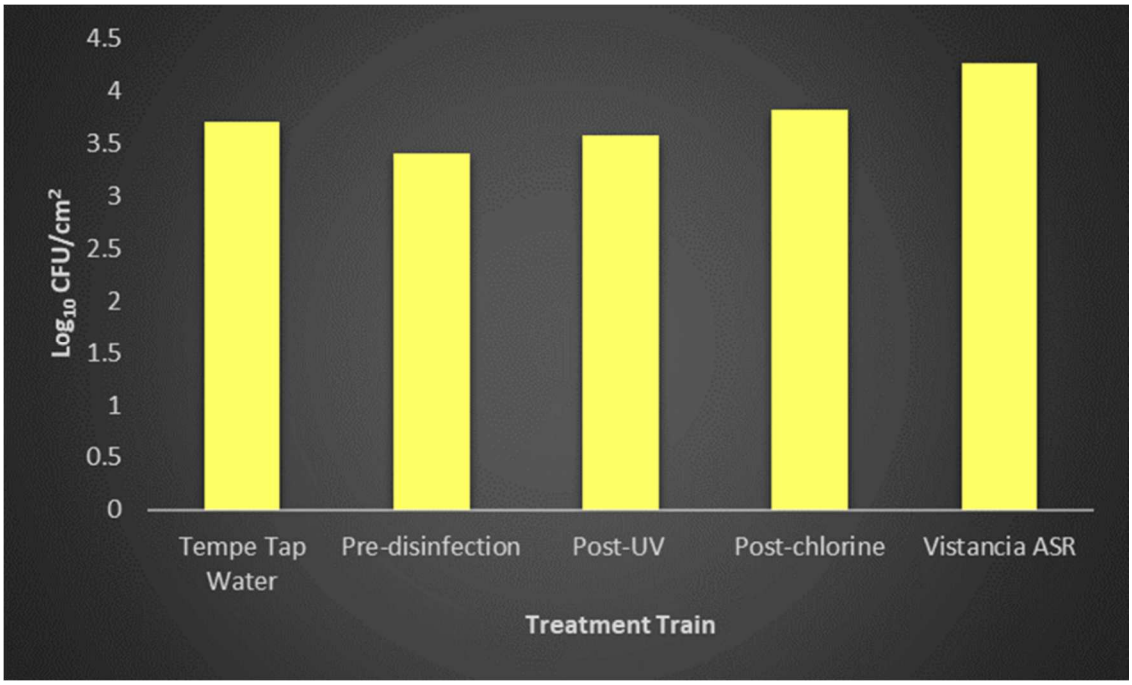

Figure 32. HPC concentration on SS304 after one-year

Galvanized steel HPC concentration after one year has some of the most unusual results. The HPC concentration decrease at the Butler Facility after each treatment train process but have the highest counts for Vistancia and ASU's microbiology laboratory (Figure 33). The high level of salts in the groundwater at Vistancia accelerate corrosion rates in galvanized steel and encourage zinc to leach out of the protective coating resulting in higher HPC concentration. The lower HPC concentrations for the Butler facility may be explained by combining UV disinfection and chlorination to remove bacteria.

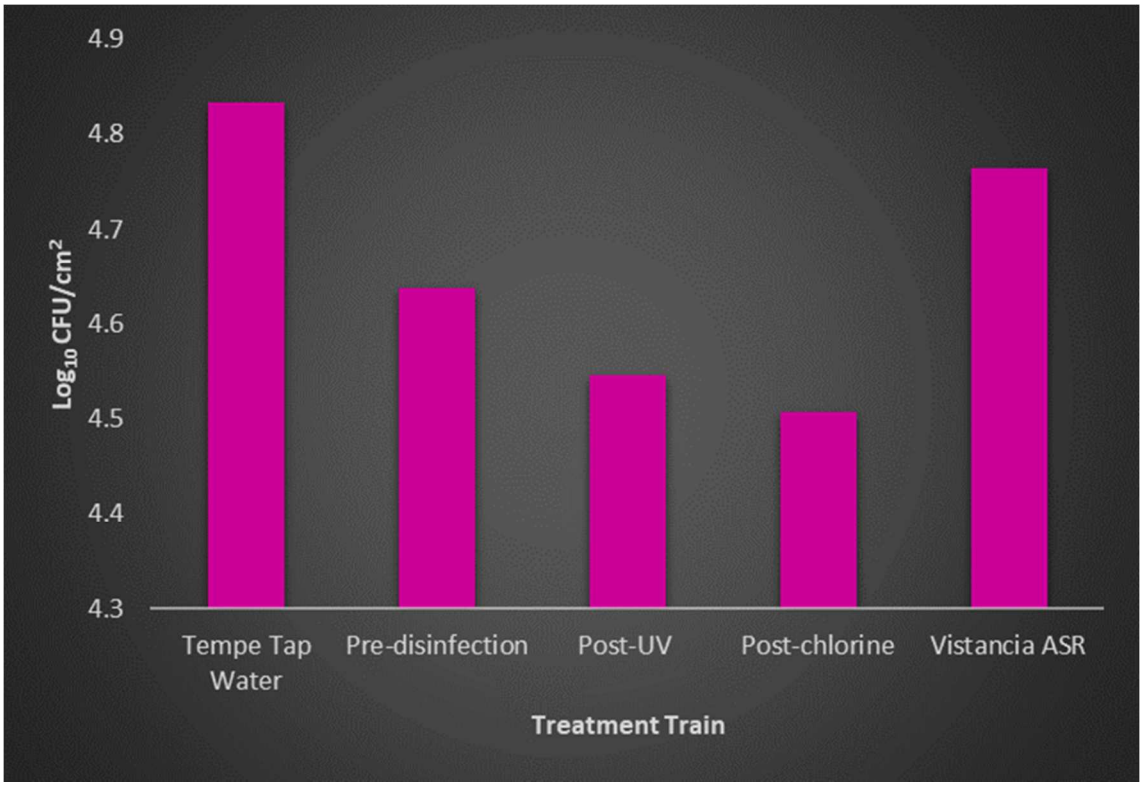

Figure 33. HPC concentration on galvanized steel after one-year

4.3 Pathogenic Bacteria

The samples were analyzed for HPC and waterborne pathogens including *Legionella* and *Mycobacterium.* The cPVC biofilm samples were used for detecting the pathogenic bacteria because cPVC does not rust. The samples indicated possible *Legionella* growth on BYCE for the one-year collection at the Butler facility but were not detected in the Vistancia one-year cPVC biofilm sample (Figure 34). The colonies are yellow, tan or white but did not fluoresce under UV light. Typically, any *Legionella* colonies should be a tan color and fluoresce if they are *Legionella pneumophila.* However, 44 tan colonies were counted on the post-UV therefore, samples were taken and stored in a freezer for later DNA analysis to confirm the presence of any *Legionella* sp. As for the *Mycobacterium* plates, there was no growth for any of the field samples

(Figure 35). The bacteria may have been able to grow by enhancing the media selectiveness for *mycobacteria* by increasing the concentration of malachite green (Hu et al. 2017). Furthermore, the plating of *Mycobacteria* on Middlebrook 7H10 agar requires the sample to be pretreated with an acid and base before plating that may need to be replaced. Middlebrook agar also needs an enrichment supplement, Oleic Albumin Dextrose Catalase, that may have been ineffective as well. Frozen samples should be reanalyzed on agar plates or by PCR to confirm or deny the presence of *Mycobacterium*.

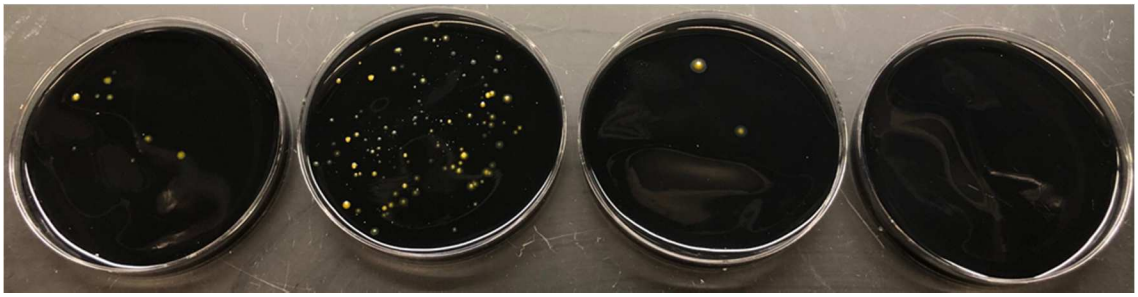

Figure 34. Bacterial colony formation on BYCE Agar for one-year cPVC field samples from pre-disinfection, post-UV, post-chlorination and Vistancia Production Well, respectively

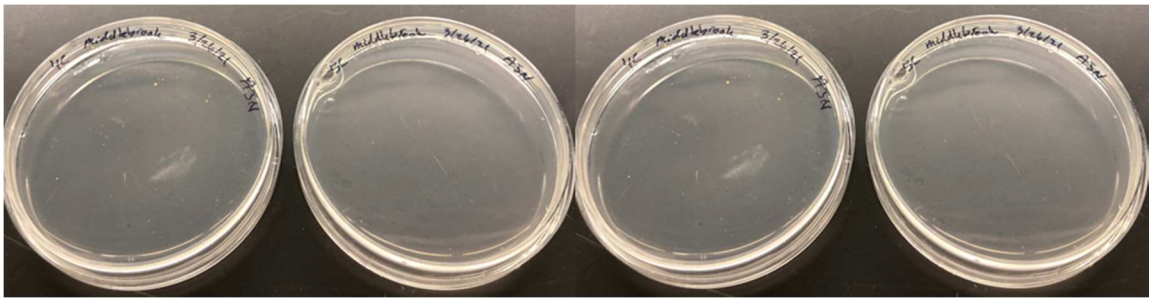

Figure 35**.** Bacteria colony formation on Middlebrook 7H10 Agar for one-year cPVC field samples from pre-disinfection, post-UV, post-chlorination, and Vistancia Production Well, respectively.

4.3 SRB

After each collection, the water from each blue sampling site location bin was collected and analyzed for SRB. Each vial from the field sampling bins contains black precipitates on the bottom of the vial with the heaviest black precipitates being from the Butler Post-Chlorination water sample (Figure 36). This means that the presence of SRB are at each location. However, the amount of precipitate does not indicate the quantity of SRB present. SRB depends on iron and sulfur in the environment. This means that water from the Butler Post-Chlorination site likely contains higher amounts of iron, as well as sulfur for survival and reproduction, but not necessarily more SRB bacteria. This is likely due to corrosive effects of UV and chlorine on iron metals which generate more available resources for SRB to survive.

Figure 36. One-year water inoculations from pre-disinfection, post-UV, post-chlorination, and Vistancia Production Well, respectively

The ability of SRBs to colonize copper at the Butler Reclamation Facility was investigated, as well. The one-year samples were collected because they displayed visible signs of corrosion in the form of Copper (II) Chloride. Furthermore, copper pipes are durable and impermeable with the added benefit of being a natural, non-toxic

antimicrobial, which is why it is so common in premise plumbing. The results show no visible indication of a black precipitate formed by SRB but show signs of growth (Figure 37). The growth is not unexpected because the samples are from a wastewater facility which is rich in a diverse community of microorganisms. Little research is available that explains MIC of copper by SRB. However, one study suggests that the growth rate of *D. vulgaris* is decreased up to 20% on copper (Cheng et al., 2004).

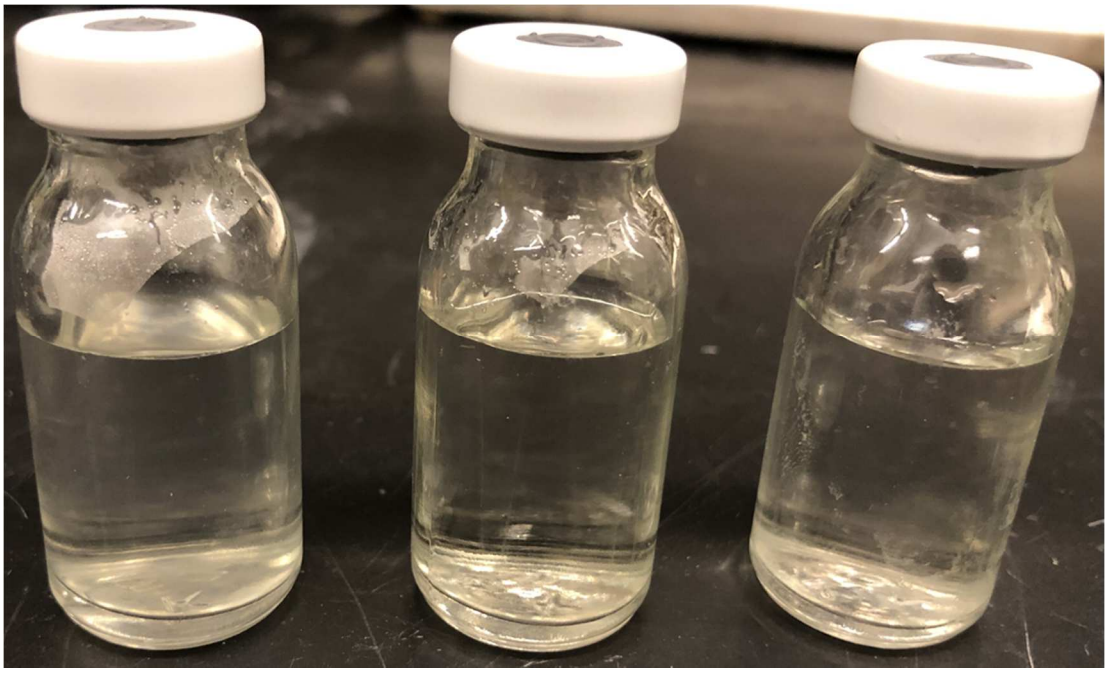

Figure 37. SRB testing vials for pre-disinfection, post-UV, and post-chlorine copper coupon biofilms after one-year

Data collected from the SRB test was processed and compiled to generate an index to predict sampling site risk of MIC by SRBs based on visually recognizable culture characteristics (Table 3). The overall risk of MIC was labeled as low, medium, or high. Low risk is defined as growth under anaerobic conditions whereas, medium risk is defined as growth under anaerobic conditions and the ability to oxidize metal. High risk of MIC is defined as growth under anaerobic conditions, the ability to oxidize metals and

the capability to form biofilms. The majority of the one and three-month samples have an overall low risk of MIC. The six-month samples suggest that the Butler Reclamation Facility is at a medium risk of MIC whereas Vistancia is at a high risk of MIC. Nearly all sampling sights are at a high risk of MIC after one year. The research lab is at the lowest risk of MIC which is expected given the lab bioreactor used potable water from a faucet that is treated with chlorine.

Table 3. Risk of MIC by SRBs based on water sample visual culture characteristics for each sampling time and location.

Treatment Train ID Site	Incubation Time (months)	SRB Growth (+/-)	Black sediment (+/-)	Polymeric sediment (+/-)	Overall Risk of MIC
Pre-Disinfection	1	+	-	-	low
Post-UV	1	+	-	-	low
Post-Chlorination	1	+	+	-	medium
Vistancia ASR	1	+	-	-	low
Tempe Tap Water	1	+	-	-	low
Pre-Disinfection	3	-	-	-	low
Post-UV	3	-	-	-	low
Post-Chlorination	3	+	-	-	low
Vistancia ASR	3	-	-	-	low
Tempe Tap Water	3	+	-	-	low
Pre-Disinfection	6	+	+	-	medium
Post-UV	6	+	-	-	low
Post-Chlorination	6	+	+	-	medium
Vistancia ASR	6	+	+	+	high
Tempe Tap Water	6	-	-	-	low
Pre-Disinfection	12	+	+	+	high
Post-UV	12	+	+	+	high
Post-Chlorination	12	+	+	+	high
Vistancia ASR	12	+	+	+	high
Tempe Tap Water	12	+	+	-	medium

Chapter 5: Conclusions

MIC is a complex phenomenon in which bacteria utilize metals and alloys for subsistence causing corrosion. The mechanisms of MIC are not well understood. However, it is widely agreed that multiple physio-chemical and microbiological factors

work together. Since MIC is not always apparent in water treatment facilities, the current methods of preventing extensive MIC damage would be by regular inspections, biocides and regular monitoring of corrosion inducing bacteria.

Ultraviolet light is used as a disinfection treatment in many water facilities due to its ability to damage genetic material, thus preventing replication of microorganisms. However, the use of UV light does not effectively penetrate biofilms and may contribute biofilm formation as well as microbial growth. Studies have shown that natural organic matter found in surface water will absorb light at 254 nm wavelength which results in larger molecules breaking down into smaller, assimilable organic matter or organic acids (Liu et al., 2006). The increase in organic acids and assimilable organic matter (AOC) may stimulate bacterial growth within the biofilm, which in return may increase corrosion rates. The heavy corrosion and thick biofilm on cast iron (Figure 14) may have inhibited the ability of AOC to diffuse within the biofilm to increase the HPC concentration, contradicting what would be expected (Figure 27). Although visible signs of rust have occurred on the galvanized steel coupons (Figure 10), the protective zinc coating is still present, consequently bacterial growth may be inhibited which could explain the lowered HPC concentration (Figure 33).

5.1 Recommendations

MIC electrochemistry and mechanisms are not straight forward. There is much to learn and understand. However, there are some ways to better control corrosion by using.

physical, chemical, or electrochemical processes. Furthermore, choosing the correct alloy for a given environment is highly effective and proven to reduce corrosion rates.

Physically controlling MIC can be laborious and must be done regularly. Pigging is a great way to remove biofilms or corrosion deposits in pipes, allowing for better water flow and to visually inspect for further damage. The use of ultraviolet (UV) radiation physically alters the genetic material of bacteria that may cause corrosion, so they are incapable of multiplying, thus deactivating them. However, UV may not be very effective against spore forming bacteria and is not effective against bacteria localized within biofilms.

Chemicals to control bacteria are known as biocides which can be broad-spectrum. While chlorine is cheap and easy to use, it is ineffective against biofilms and reacts with organic matter which can result in hazardous chemical compounds forming. Chloramines can penetrate biofilms, are less corrosive and less toxic, but cost more than chlorine and is less effective than chlorine (Javaherdashti, 2018).

Electrochemical methods of MIC control is a relatively new concept. This mainly involves protecting the cathodes and coatings. Studies have shown that applying a voltage of -0.95v to a reference electrode may protect against SRB-induced corrosion (Javaherdashti, 2018). However, it is difficult to produce consistent results and has been shown not to work every time. Thus, more research is needed on cathode protection. Coatings on the other hand are very common and consistently protect against corrosion if the coating is well maintained. These coatings may be polymer based or silicone based. Other coatings are an epoxy resin which contain anti-microbial copper shavings

(Javaherdashti, 2018). Though easy to use, if neglected those coatings can easily encourage bacterial growth.

Selecting the correct metal or alloy for the specific environment is the best way to reduce corrosion rates. There are many factors to consider when selecting an appropriate material type, especially when chloride and alkaline environments are present as they are notorious for accelerating SCC. Other factors to consider include the current type of corrosion being experienced and the type of acid that may be present as shown in Table 2.

Table 4. Alloy corrosion susceptibility based on environmental factors (Prowato, 2009).

Environment	Problem	Poor	Good	Best
Chlorides	Pitting, crevice corrosion	300 Series SS	Duplex alloys 317L	Alloy 276
Chlorides/Halides	Stress corrosion cracking	300 Series SS	Duplex alloys	Alloy 600/625
Hydrochloric Acid	Pitting, crevice corrosion	Titanium, Duplex, 20 Cb-3	Alloy 22, 276	Zirconium, Tantalum
Hydrofluoric Acid	Pitting, crevice corrosion	Duplex Alloys	Silver, Gold	Copper, Alloy 400
Sulfuric Acid	Pitting, crevice corrosion	Copper-Nickel (Alloy 601)	20 Cb-3	Alloy 622
General Acidic Attack	Critical Pitting	300 Series SS	317L Duplex Alloys	Alloy 25-6 Mo Alloy 625

5.2 Future Work

Microbial induced corrosion is understudied, and its mechanisms are not well understood. It is apparent that the type of corrosion depends on the media and microbes present. To better understand the causes of corrosion at the treatment facility the type of corrosion should be examined by using a scanning electron microscope to determine whether pitting, crevice, or stress cracking corrosion is occurring. The specific types of

microbes causing the accelerated corrosion along with any symbiotic relationship the sulfur reducing bacteria may have with iron oxidizing or iron reducing bacteria should be investigated, as well. Furthermore, water chemistry should be analyzed to understand the impact the ions and corrosive media have on the materials used at a specific facility. Lastly, molecular analysis should be conducted to verify specific species of bacteria present in these corrosive environments to establish which treatment and prevention option is appropriate for the treatment facility.

REFERENCES

Amha, Y. M., Anwar, M. Z., Kumaraswamy, R., Henschel, A., & Ahmad, F. (2017). Mycobacteria in Municipal wastewater treatment and REUSE: Microbial diversity for screening the occurrence of clinically and Environmentally relevant species in arid regions. Retrieved April 14, 2021, from https://pubmed.ncbi.nlm.nih.gov/28139909/

Banerjee, D., Shivapriya, P.M., Gautam, P.K. *et al.* (2020). A Review on Basic Biology of Bacterial Biofilm Infections and Their Treatments by Nanotechnology-Based Approaches. *Proc. Natl. Acad. Sci., India, Sect. B Biol. Sci.* **90**, 243–259. https://doi.org/10.1007/s40011-018-01065-7

Caicedo, C., Beutel, S., Scheper, T., Rosenwinkel, K. H., & Nogueira, R. (2016). Occurrence of legionella in wastewater treatment plants linked to wastewater characteristics. Retrieved April 14, 2021, from https://pubmed.ncbi.nlm.nih.gov/27376367/

Chang, In Seop et al. (2004). "Differential expression of Desulfovibrio vulgaris genes in response to Cu(II) and Hg(II) toxicity." Applied and environmental microbiology vol. 70,3: 1847-51. doi:10.1128/AEM.70.3.1847-1851.2004

Chen, Tianyuan, et al. (2022). "Changes in Wastewater Treatment Performance and the Microbial Community during the Bioaugmentation of a Denitrifying Pseudomonas Strain in the Low Carbon–Nitrogen Ratio Sequencing Batch Reactor." *Water*, vol. 14, no. 4, 2022, p. 540., https://doi.org/10.3390/w14040540.

"City of Peoria." *Water Resources and Quality | City of Peoria*, June 2020, www.peoriaaz.gov/government/departments/water-services/water-resources.

"City of Tempe, AZ." *General Water Quality Information | City of Tempe, AZ*,2020, www.tempe.gov/government/municipal-utilities/water/water-quality/general-water-quality-information.

Hu, Yuli et al. (2017). "Isolation of nontuberculous mycobacteria from soil using Middlebrook 7H10 agar with increased malachite green concentration." *AMB Express* vol. 7,1 (2017): 69. doi:10.1186/s13568-017-0373-6

IHS Markit. (2019, May). Ferric Chloride: Chemical economics Handbook. Retrieved April 23, 2021, from https://ihsmarkit.com/products/ferric-chloride-chemical-economics-handbook.html

Javaherdashti, R. (2018). *Microbiologically Influence Corrosion: An Engineering Insight*. Springer-Verlag.

Jia, R., Yang, D., Xu, D., & Gu, T. (2017). Electron transfer mediators accelerated the microbiologically influence corrosion against carbon steel by nitrate reducing Pseudomonas aeruginosa biofilm. *Bioelectrochemistry,118*, 38-46. doi:https://doi.org/10.1016/j.bioelechem.2017.06.013.

Jyoti, Dhrubo. (2021).“No Manual Scavenging Deaths, 941 Died While Cleaning Sewers: Govt.” *Hindustan Times*, 5 Aug. 2021, www.hindustantimes.com/india-news/no-manual-scavenging-deaths-941-died-while-cleaning-sewers-govt-101628105749227.html.

“Legionella Bacteria.” *Legionella.org*, Janet E. Stout, 27 July 2020, https://legionella.org/about-the-disease/what-is-legionnaires-disease/legionella-bacteria/

Lettinga, Kamilla D et al. (2002). “Health-related quality of life and posttraumatic stress disorder among survivors of an outbreak of Legionnaires disease.” *Clinical infectious diseases : an official publication of the Infectious Diseases Society of America* vol. 35,1 (2002): 11-7. doi:10.1086/340738

Liu, W., Cheung, L.-M., Yang, X., & Shang, C. (2006). *Thm, HAA and cncl formation from UV irradiation and chlor(am)ination of selected organic waters*. Water Research. https://www.sciencedirect.com/science/article/pii/S0043135406001734

Lv, M., & Du, M. (2018). A review: Microbiologically influenced corrosion and the effect of cathodic polarization on typical bacteria. *Reviews in Environmental Science and Bio/Technology,17*(3), 431-446. doi:10.1007/s11157-018-9473-2

Makhlouf, A. H., & Botello, M. A. (2018). *Chapter 1- Failure of the Metallic Structures Due to Microbiologically Induced Corrosion and the Techniques for Protection,* 1-18. Retrieved December 2, 2020, from https://www.sciencedirect.com/science/article/pii/B978008101928300001X.

Ming, L.C. (2021). Legionella pneumophila — The causative agent of Legionnaires' disease - Scientific Figure on ResearchGate. Available from: https://www.researchgate.net/figure/The-transmission-sources-life-cycle-within-water-systems-and-human-macrophage-the_fig1_350761825 [accessed 19 Dec, 2021].

Natarajan, K.A. (2018). “Biofouling and Microbially Influenced Corrosion.” *Biotechnology of Metals*, Elsevier, 15 June 2018, www.sciencedirect.com/science/article/pii/B9780128040225000128.

Porcheron G, Garenaux A, Proulx J, Sabri M and Dozois CM (2013) Iron, copper, zinc, and manganese transport and regulation in pathogenic Enterobacteria: correlations between strains, site of infection and the relative importance of the different metal transport systems for virulence. *Front. Cell. Infect. Microbiol*. **3**:90. doi: 10.3389/fcimb.2013.00090

Prawoto, Yunan, et al. “Effect of Ph and Chloride Concentration on the Corrosion of Duplex Stainless Steel.” *Research Gate*, Arabian Journal for Science and Engineering , Dec. 2009, www.researchgate.net/publication/238739911_Effect_of_ph_and_chloride_concentration_on_the_corrosion_of_duplex_stainless_steel#pf6.

The Republic . “Scottsdale Police Identify 2 Workers Who Died in Sewer.” *The Arizona Republic*, The Republic | Azcentral.com, 27 Aug. 2014,

www.azcentral.com/story/news/local/scottsdale/2014/08/26/scottsdale-sewage-vault-victims-abrk/14629257/.

Tao, X., Li, Y., Huang, H. *et al. Desulfovibrio vulgaris* Hildenborough prefers lactate over hydrogen as electron donor. *Ann Microbiol* 64, 451–457 (2014). https://doi.org/10.1007/s13213-013-0675-0

Trenchless Technology. (2019). Infrastructure Corrosion Is a Major Threat to Public Health, Says Study. Retrieved April 12, 2021, from https://trenchlesstechnology.com/nace-report-identifies-corrosion-as-major-threat-to-public-health/

Tripathi, A. K., et al. (2021). Gene Sets and Mechanisms of Sulfate-Reducing Bacteria Biofilm Formation and Quorum Sensing With Impact on Corrosion. *Frontiers in microbiology*, *12*, 754140. https://doi.org/10.3389/fmicb.2021.754140

Trigodet F, Larché N, Morrison HG, Jebbar M, Thierry D, Maignien L. Electroactive Bacteria Associated With Stainless Steel Ennoblement in Seawater. Frontier in Microbiology. 2019 Feb 7.